NAVAL POSTGRADUATE SCHOOL
Monterey, California

THESIS

DEVELOPMENT AND CONTROL OF THE NAVAL POSTGRADUATE SCHOOL PLANAR AUTONOMOUS DOCKING SIMULATOR (NPADS)

by

Robert D. Porter

September 2002

Thesis Advisor:	Michael G. Spencer
Second Reader:	Brij N. Agrawal

Approved for public release; distribution is unlimited

THIS PAGE INTENTIONALLY LEFT BLANK

REPORT DOCUMENTATION PAGE			*Form Approved OMB No. 0704-0188*
Public reporting burden for this collection of information is estimated to average 1 hour per response, including the time for reviewing instruction, searching existing data sources, gathering and maintaining the data needed, and completing and reviewing the collection of information. Send comments regarding this burden estimate or any other aspect of this collection of information, including suggestions for reducing this burden, to Washington headquarters Services, Directorate for Information Operations and Reports, 1215 Jefferson Davis Highway, Suite 1204, Arlington, VA 22202-4302, and to the Office of Management and Budget, Paperwork Reduction Project (0704-0188) Washington DC 20503.			
1. AGENCY USE ONLY ***(Leave blank)***	**2. REPORT DATE** September 2002	**3. REPORT TYPE AND DATES COVERED** Master's Thesis	
4. TITLE AND SUBTITLE: Development and Control of the Naval Postgraduate School Planar Autonomous Docking Simulator (NPADS)			**5. FUNDING NUMBERS**
6. AUTHOR(S) Robert D. Porter			
7. PERFORMING ORGANIZATION NAME(S) AND ADDRESS(ES) Naval Postgraduate School Monterey, CA 93943-5000			**8. PERFORMING ORGANIZATION REPORT NUMBER**
9. SPONSORING /MONITORING AGENCY NAME(S) AND ADDRESS(ES) N/A			**10. SPONSORING/MONITORING AGENCY REPORT NUMBER**
11. SUPPLEMENTARY NOTES The views expressed in this thesis are those of the author and do not reflect the official policy or position of the Department of Defense or the U.S. Government.			
12a. DISTRIBUTION / AVAILABILITY STATEMENT Approved for public release; distribution is unlimited			**12b. DISTRIBUTION CODE**

13. ABSTRACT ***(maximum 200 words)***

The objective of this thesis was to design, construct and develop the initial autonomous control algorithm for the NPS Planar Autonomous Docking Simulator (NPADS). The effort included hardware design, fabrication, installation and integration; mass property determination; and the development and testing of control laws utilizing MATLAB and Simulink for modeling and LabView for NPADS control.

The NPADS vehicle uses air pads and a granite table to simulate a 2-D, drag-free, zero-g space environment. It is a completely self-contained vehicle equipped with eight cold-gas, bang-bang type thrusters and a reaction wheel for motion control. A "star sensor" CCD camera locates the vehicle on the table while a color CCD docking camera and two robotic arms will locate and dock with a target vehicle. The on-board computer system leverages PXI technology and a single source, simplifying systems integration. The vehicle is powered by two lead-acid batteries for completely autonomous operation.

A graphical user interface and wireless Ethernet enable the user to command and monitor the vehicle from a remote command and data acquisition computer. Two control algorithms were developed and allow the user to either control the thrusters and reaction wheel manually or simply specify a desired location and rotation angle.

14. SUBJECT TERMS Attitude determination, Attitude control, LabView, MATLAB, SIMULINK, Autonomous docking, Satellite simulator, Pulse Width Modulation thruster control			**15. NUMBER OF PAGES** 101
			16. PRICE CODE
17. SECURITY CLASSIFICATION OF REPORT Unclassified	**18. SECURITY CLASSIFICATION OF THIS PAGE** Unclassified	**19. SECURITY CLASSIFICATION OF ABSTRACT** Unclassified	**20. LIMITATION OF ABSTRACT** UL

NSN 7540-01-280-5500 Standard Form 298 (Rev. 2-89)
Prescribed by ANSI Std. 239-18

THIS PAGE INTENTIONALLY LEFT BLANK

Approved for public release; distribution is unlimited

DEVELOPMENT AND CONTROL OF THE NAVAL POSTGRADUATE SCHOOL PLANAR AUTONOMOUS DOCKING SIMULATOR (NPADS)

Robert D. Porter
Lieutenant Commander, United States Navy
B.S., Penn State University, 1989

Submitted in partial fulfillment of the
requirements for the degree of

MASTER OF SCIENCE IN ASTRONAUTICAL ENGINEERING

from the

NAVAL POSTGRADUATE SCHOOL
September 2002

Author: Robert D. Porter

Approved by: Michael G. Spencer, Thesis Advisor

Brij N. Agrawal, Second Reader

Max F. Platzer, Chairman
Department of Aeronautics and Astronautics

THIS PAGE INTENTIONALLY LEFT BLANK

ABSTRACT

The objective of this thesis was to design, construct and develop the initial autonomous control algorithm for the NPS Planar Autonomous Docking Simulator (NPADS). The effort included hardware design, fabrication, installation and integration; mass property determination; and the development and testing of control laws utilizing MATLAB and Simulink for modeling and LabView for NPADS control.

The NPADS vehicle uses air pads and a granite table to simulate a 2-D, drag-free, zero-g space environment. It is a completely self-contained vehicle equipped with eight cold-gas, bang-bang type thrusters and a reaction wheel for motion control. A “star sensor” CCD camera locates the vehicle on the table while a color CCD docking camera and two robotic arms will locate and dock with a target vehicle. The on-board computer system leverages PXI technology and a single source, simplifying systems integration. The vehicle is powered by two lead-acid batteries for completely autonomous operation.

A graphical user interface and wireless Ethernet enable the user to command and monitor the vehicle from a remote command and data acquisition computer. Two control algorithms were developed and allow the user to either control the thrusters and reaction wheel manually or simply specify a desired location and rotation angle.

THIS PAGE INTENTIONALLY LEFT BLANK

TABLE OF CONTENTS

LIST OF FIGURES

LIST OF TABLES

THIS PAGE INTENTIONALLY LEFT BLANK

ACKNOWLEDGMENTS

The author would like to thank the following people for their invaluable assistance in the completion of this thesis:

Prof. Michael Spencer & Brij Agrawal - For their outstanding sponsorship and guidance.

Air Force Research Lab (AFRL) – For their outstanding support and sponsorship.

LT Gary Cave – For his friendship and partnership in completing the NPADS vehicle.

CDR Bill Erhardt – For his work on the NPADS Vision System.

Mr. Jerry Lentz – For building the power distribution system.

Mr. Glen Harrell – For building the NPADS frame and numerous other structural components.

Mr. Ron Phelps – For building the reaction wheel shunt.

And most importantly to my wife Holly, for putting up with another school and supporting everything I do with limitless love and devotion.

THIS PAGE INTENTIONALLY LEFT BLANK

I. INTRODUCTION

A. BACKGROUND

1. On-Orbit Docking and Servicing

On orbit docking and servicing of spacecraft has been an area of research and development since the early manned space missions. Space vehicle docking was first accomplished during the Gemini program in 1966 and has progressed to the current Shuttle-Mir and Shuttle-Space Station systems. Robotic operations in space have also been developed with the Shuttle Remote Manipulator System (SRMS) and the Space Station Remote Manipulator System (SSRMS); however, these systems were developed for large space vehicles (10,000's kg) and require a man-in-the-loop.

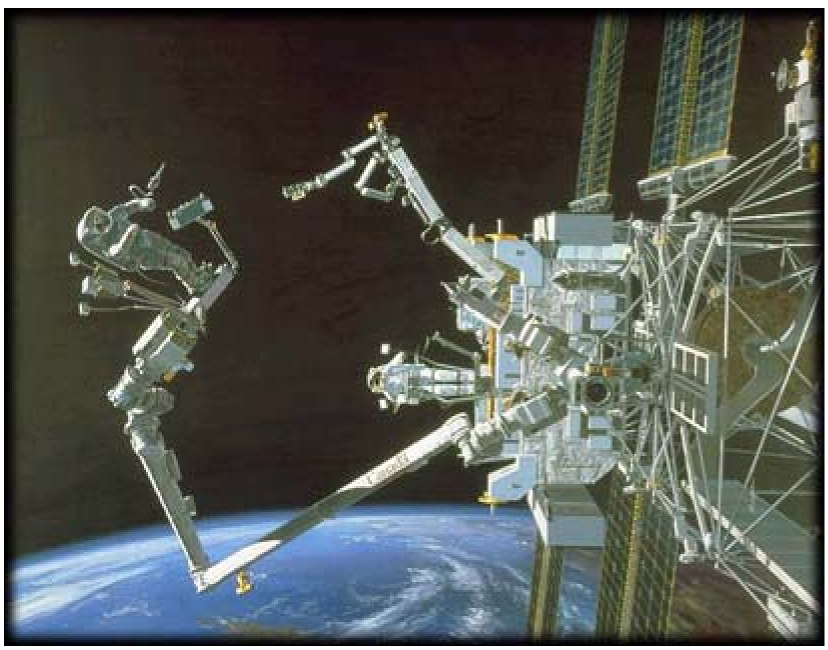

Figure 1 Space Station Remote Manipulator System (SSRMS) (From Ref. 1)

Currently unmanned space systems are being designed smaller and built faster to provide a more responsive capability for payload customers. The Air Force, NRO, and NASA have several space missions in development, using several small spacecraft instead of single large vehicles. Developing the capability to refuel and service these smaller spacecraft on-orbit can greatly extend the usefulness and lifetime of the mission.

Exploitation of robotic techniques can provide the needed capabilities for fully autonomous on-orbit fueling, modification and simple assembly in space.

The development of smaller, more versatile spacecraft has added a new focus for research into autonomous space robots and space manipulator systems capable of interfacing with vehicles in the 100's kg scale. Future space robotic systems must possess capabilities beyond those of the SRMS, which operated at low speeds as a single robotic arm linked to its massive Shuttle base.

The next generation of space robots and space manipulators will also involve smaller servicing vehicles similar in size to the receiver vehicles. When the manipulator "base" spacecraft is comparable in mass and moments of inertia to the manipulator-plus-payload, the reactive base motions will be significant, complex and highly nonlinear. The robotic methods and systems used in the Shuttle and SRMS are no longer sufficient or applicable to the new small spacecraft robotic servicing tasks of the future. Reliable space-based manipulator operations therefore require new control strategies that consider the uncertain external environment of space while also accounting for the complex spacecraft-manipulator dynamic coupling.

NASA is completing work on the Autonomous Extravehicular Robotic Camera (AERCam Spirit), Figure 2, with the goal of creating a "nanosatellite" for assisting astronauts during Extravehicular Activities (EVA). This program demonstrates the enormous potential for using miniature satellites for on-orbit servicing but still requires a man-in-the-loop for control [Ref. 1].

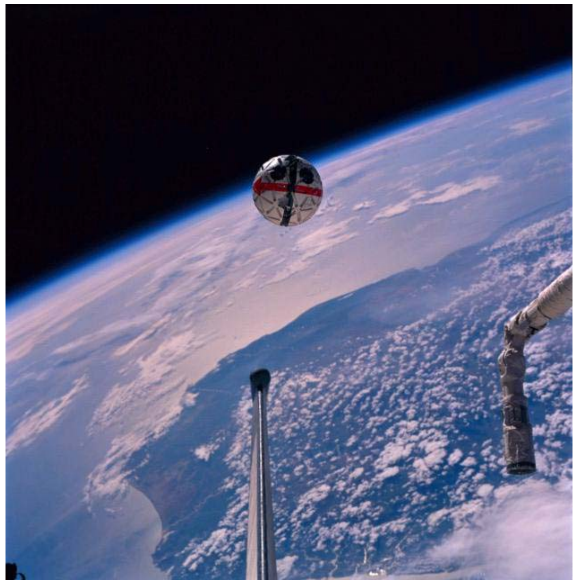

Figure 2 NASA AERCam Spirit (From Ref. 1)

A major contributor in the development of autonomous docking technology was the Engineering Test Satellite VII (ETS-VII) mission, Figure 3. Developed and launched by the National Space Development Agency of Japan (NASDA), the ETS-VII mission consisted of a main satellite and target satellite launched together in the docked configuration. Once on orbit, the two spacecraft were separated and demonstrated the control techniques necessary for autonomous docking and the visual servo-tracking of a 6 degree of freedom manipulator hand. While completely autonomous target capture and docking were not demonstrated, the required technologies were verified and it paved the way for future development [Ref. 2].

Figure 3 Engineering Test Satellite VII (ETS-VII) (From Ref. 2)

As part of the NASA Space Launch Initiative, Orbital Science Corporation is developing the Demonstration of Autonomous Rendezvous Technology (DART). DART will include the location and docking of a target spacecraft without direct human guidance. Launched aboard a Pegasus rocket, the vehicle will perform several orbit transfers to arrive near the target satellite using GPS relative navigation. The vehicle will approach the target within 15 meters before continuing to a final orbit [Ref. 3]. The DART Mission Profile is depicted in Figure 4.

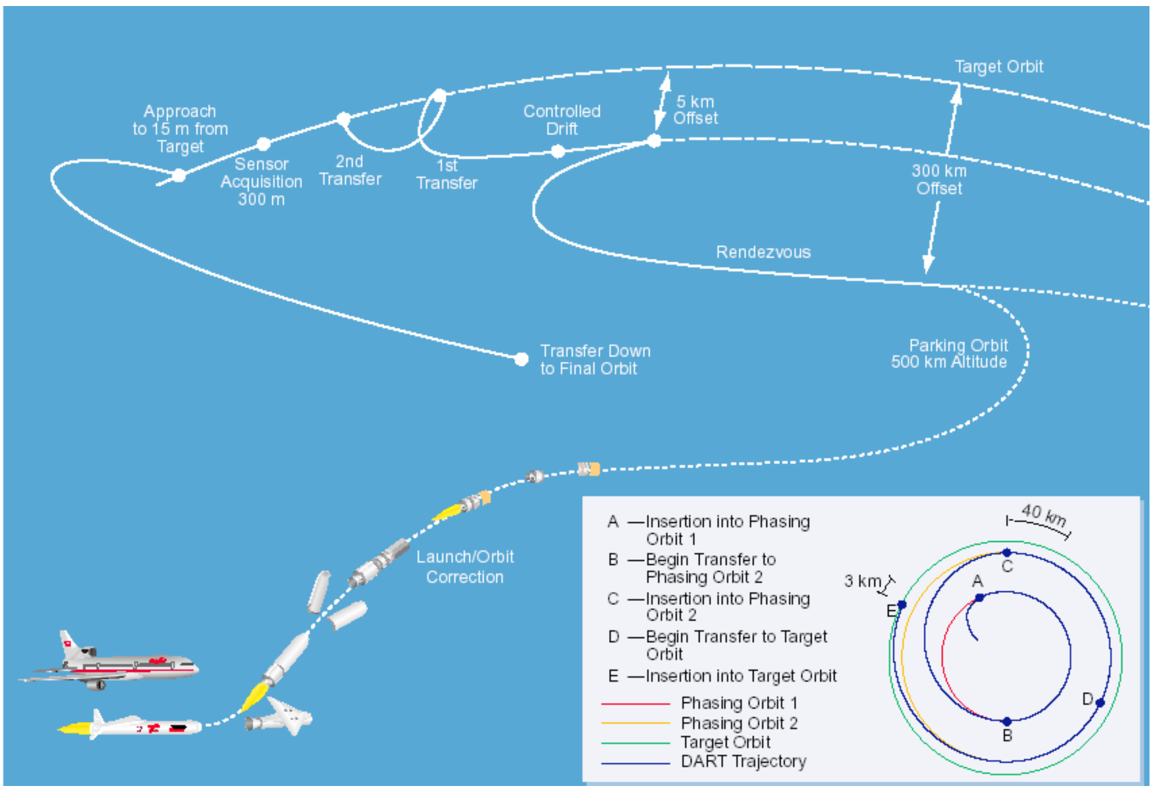

Figure 4 DART Mission Profile (From Ref. 2)

Satellite servicing has become a new subject of considerable interest to the DoD. The Air Force Research Laboratory in Kirtland, NM has a group that has started an effort to identify the technologies and systems necessary to develop and implement satellite refueling and servicing of military spacecraft. In addition, DARPA has initiated the "Orbital Express" mission as a means of demonstrating many of the current technologies for refueling and servicing. Phase I efforts were awarded to three contractor teams and the work began in October 2000. The Phase II efforts are to culminate in an on-orbit demonstration of rendezvous, docking and servicing in the year 2004. It is anticipated that upon a successful completion of that mission, the task of satellite servicing for the DoD will be turned over to the Air Force for further development and implementation. The significance of the NPS Planar Autonomous Docking Simulator is that it will benefit the Navy and Air Force by providing a new development tool and validation test-bed for future small satellite servicing technologies and systems.

2. Spacecraft Research and Design Center

The Spacecraft Research and Design Center (SRDC) at the Naval Postgraduate School (NPS) consists of four laboratories and a reference library. One of these laboratories, the Satellite Servicing Laboratory, was host to this experimental research. The NPS Planer Autonomous Docking Simulator was designed to be the focal research area within the Satellite Servicing Laboratory and is funded by the Air Force Research Laboratory in Albuquerque, New Mexico.

B. NPS PLANAR AUTONOMOUS DOCKING SIMULATOR (NPADS)

The objective of this research is to develop an autonomous servicing spacecraft simulator and test-bed. The simulator will be used for the development and validation of autonomous control algorithms as well as various hardware elements necessary for autonomous rendezvous and docking, space manipulator control, and satellite servicing operations. The NPADS design concept is depicted in Figure 5.

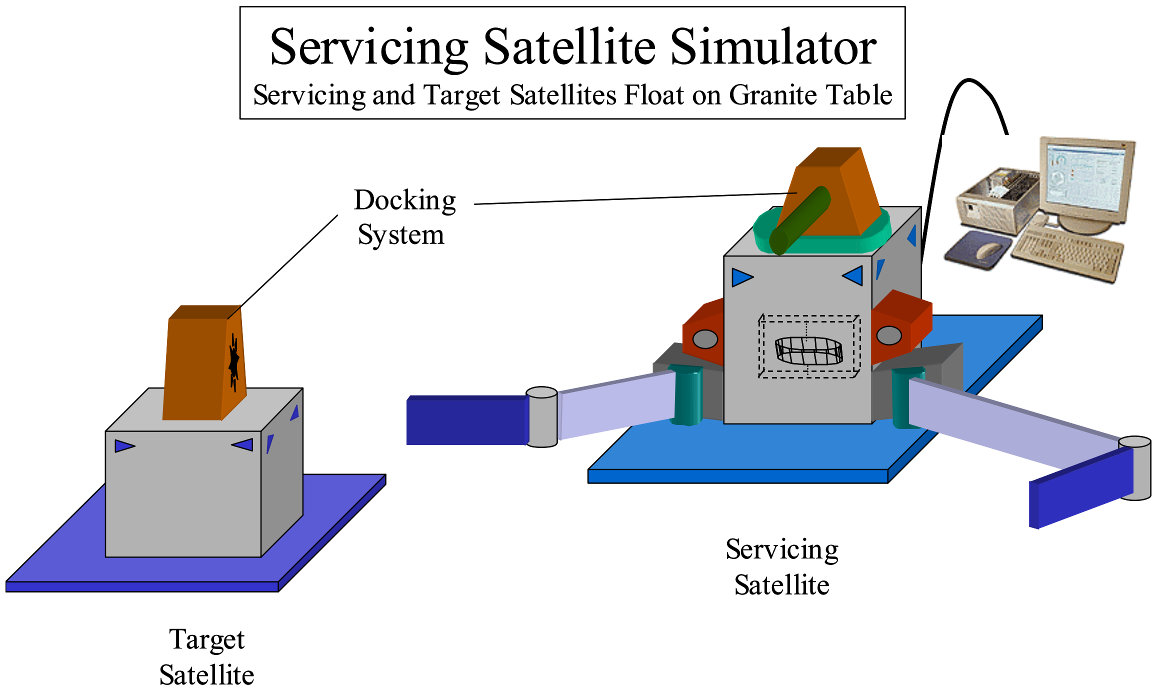

Figure 5 NPADS Design Concept

1. Hardware

NPADS will consist of a servicing vehicle and a target vehicle, both floating on an air bearing granite table to simulate a two dimensional space environment. The servicing vehicle includes a color CCD camera and two robotic arms for target acquisition, capture and docking. The Attitude determination and control system consists of a "star sensor" CCD camera, MEMS angular rate sensor, eight cold-gas, bang-bang type thrusters and a reaction wheel. The target vehicle, while not completely developed at this time, will consist of a reaction wheel, to spin the vehicle, and a control computer for data acquisition and docking mechanism control. Both vehicles use onboard lead-acid batteries for completely autonomous operation.

2. Software

The control software for the servicing vehicle was developed using the National Instruments LabView software package. All of the user interfaces and data acquisition occur via a wireless Ethernet system. Initial simulation and modeling was accomplished using Mathworks MATLAB/SIMULINK.

C. SCOPE OF THESIS

This thesis comprises the work involved in the design, construction and initial programming of the NPADS servicing vehicle. It is the first phase in the development of a fully autonomous, neural network based, rendezvous and docking simulator.

Following several weeks of design research, the vehicle was constructed and the individual components integrated. This required the creation of numerous wiring harnesses, a power distribution system, and a thruster and flotation air distribution system. Once the hardware was constructed, each system was integrated with a control computer and a manual control system was developed to test each component of the design. Simultaneously, a Simulink model of the control scheme was developed to test the required pulse width modulation code for thruster control. Following successful modeling, a PD controller was developed and tested.

THIS PAGE INTENTIONALLY LEFT BLANK

II. NPADS HARDWARE

NPADS was designed in layers with a focus on the ability to easily repair or replace components throughout the life of the project. During design and testing, NPADS was completely dismantled and rebuilt several times in less than two hours. This chapter describes the individual hardware components used in the design of NPADS, their operation and the overall layout as depicted in Figure 6.

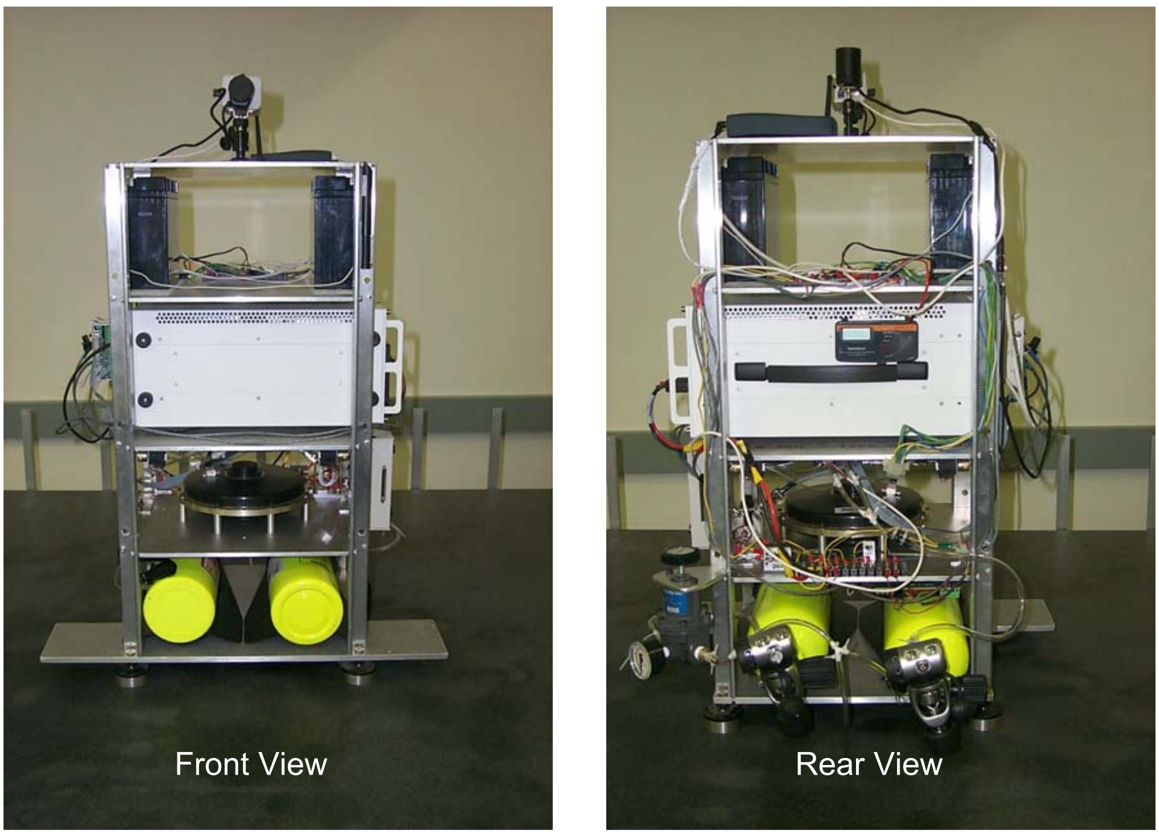

Figure 6 NPS Planar Autonomous Docking Simulator

A. OVERVIEW

One of the primary objectives in the design of NPADS was to create an autonomous docking simulator using commercially available components that require little or no modification prior to installation and use. The focus from the start of the project was to get NPADS operational as soon as possible so that it could be used for follow-on research. In addition, NPADS was design to operate on a 6x8 ft granite table, limiting the size of the vehicle.

NPADS consists of 5 levels. Each level contains most, if not all, of the components for a major subsystem of the design. Table 1 lists each level and the subsystem it supports.

Table 1 NPADS Subsystems

Shelf	Subsystem
Base	Floatation / Air Supply System
1	Propulsion / Control System
2	Computer System
3	Power System / Docking System[1]
4	Vision System

(1) To be incorporated during follow-on research

In order to simulate a two dimensional space environment, NPADS floats on an air-bearing table via four air pads connected to the underside of the first level. A camera, mounted on the forth shelf, is used as a star sensor to provide two-dimensional spatial position on the table. Gross attitude control is accomplished using eight cold-gas thrusters mounted on the underside of the second shelf. For fine attitude control and docking, NPADS will use a reaction wheel mounted on the first shelf. The reaction wheel is operational but unused in the control of the vehicle. Chosen for its modular instrumentation design and simple systems integration, a National Instruments PXI computer system is at the heart of the NPADS spacecraft. All of the required data acquisition systems are contained in a single chassis on the second shelf. Labview was chosen as the programming language for its advanced graphical user interface and the ability to leverage work being done by other Labview users in academia and industry. It was used to program all data acquisition / control. Table 2 contains a summary of the major NPADS characteristics.

Table 2 NPADS Major System Characteristics

	Parameter	Value
Physical Size	Length	15 in
	Width[1]	15 in
	Height[2]	36 in
	Mass	142 lbm
Propulsion / Control System	Actuator Type	Cold-Gas Thrusters
	Propellant	Compressed Air
	Storage Capacity	19 ft^3
	Operating Pressure	0-150 psi
	Continuous Operation[3]	20 min
	Thruster Force[4]	0.076 lbf (0.34 N)
	Reaction Wheel	2.5 N-m-s
Electrical System	Battery Type	Lead-Acid
	Storage Capacity	20 Ah @ 12Vdc
	Continuous Operation[5]	45 min
	Regulated Voltages	±5, 6, 12, 18, 24 Vdc
Computer System	Computer	National Instruments PXI
	Processor	866 MHz PIII
	Data Acquisition Cards	Analog / Digital / Vision
	Power	24 Vdc / AC
Vision System	Star Sensor Camera	Provideo Bullet CCD
	Shutter Speed	100 Hz
	Docking Camera	Sanyo color CCD
	Shutter Speed	250 Hz

1. Width is 25 in. with arm pads included.
2. Height includes "Star sensor" camera.
3. Operating time will vary based on thruster workload.
4. At 150 psi. operating pressure.
5. Operating time will vary with number of systems operational and workload.

B. STRUCTURES

1. Frame

The NPADS frame is constructed of 6061-T6 Aluminum and provides the support structure for all of the required systems. It consists of a 3/8-inch thick base plate and four 1/4-inch thick shelves, each supported by four 1/4-inch angle risers. (Figure 7) Each shelf is 15x15 inches and weighs approximately 5-1/2 lbs. The base plate, which includes two 5x5 inch arm-mounting pads extending from the first 5 inches of the left and right side, weighs approximately 10 lbs. When fully assembled, the frame stands 2-feet 5-1/2 inches tall and weighs 32 lbs (14.5 kg). The frame is connected using 1/2-inch long 10/32 screws.

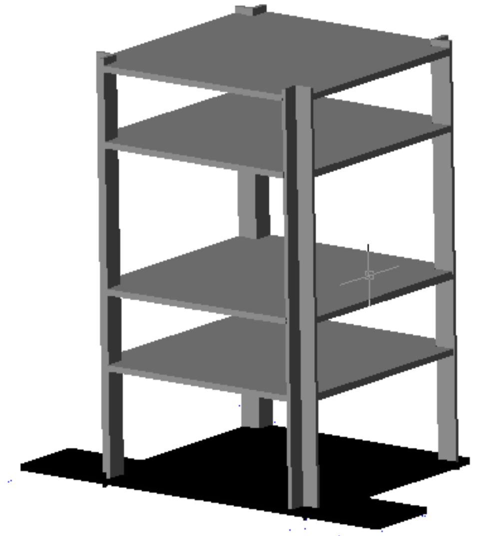

Figure 7 NPADS Frame

C. FLOATATION / AIR SUPPLY SYSTEM

1. Air Pads

Four air pads connected to the frame base plate support the entire docking simulator and provide near frictionless operation on an air-bearing table (Figure 8).

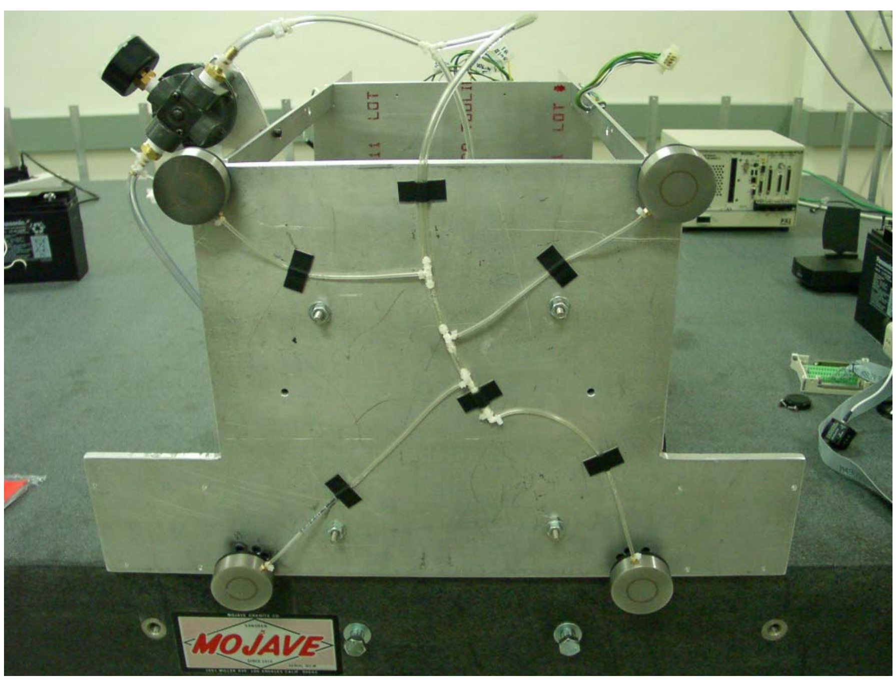

Figure 8 NPADS Air Pads

The air pads, manufactured by Aerodyne Belgium, are 2-1/8 inches (55mm) in diameter and will provide a 20-micron air gap between each pad and the table with a supply pressure of 58 psi. Air is supplied to each pad from the air supply system through 1/16 ID x 1/8 OD tubing connected to a hose fitting on the side of the pad.

2. Compressed Air Supply System

Air is provided to each of the four air pads and eight thrusters from two separate 19 cu.ft. aluminum scuba tanks. The 3000-psi air pad tank pressure is reduced to 150 psi by a standard dive regulator prior to entering a pressure regulators mounted on the aft corner of the simulator (Figure 9). The pressure regulator can be set anywhere between 0-150 psi depending on simulator weight. The air pad supply tank will provide enough air for approximately 40 minutes of operation at 50 psi. Depending on thruster workload and pressure, the thruster supply tank will provide for approximately 20 minutes of continuous operation. The air supply system is connected by 1/4 ID x 3/8 OD polyurethane tubing up to the pressure regulator and 1/8 ID x 1/4 OD and 1/16 ID x 1/8 OD tubing from the regulator to the individual air pads and thrusters.

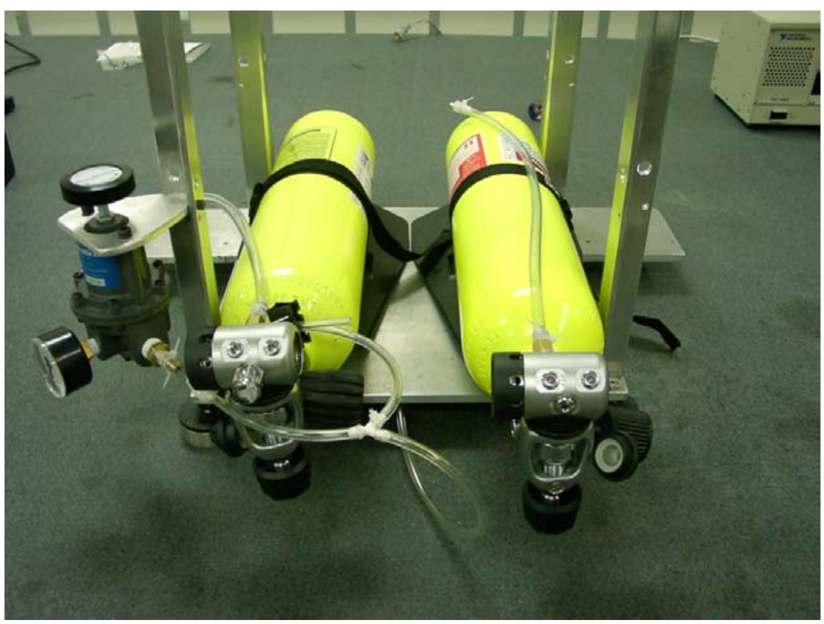

Figure 9 Air Supply System

D. POWER

Two 12-volt, 20 Ah Lead-Acid batteries are connected in series on the forth level, as depicted in Figure 10, to provide the 24-volt dc power required for simulator operation. During the design phase, lead-acid batteries were chosen due to their low cost, simple maintenance and longer duty cycle. A Radio Shack pocket voltmeter is mounted to the side of the computer chassis to monitor battery state. NPADS should not be operated without external power to the computer below 21 vdc, as indicated on the voltmeter, due to the possibility of power loss to the computer.

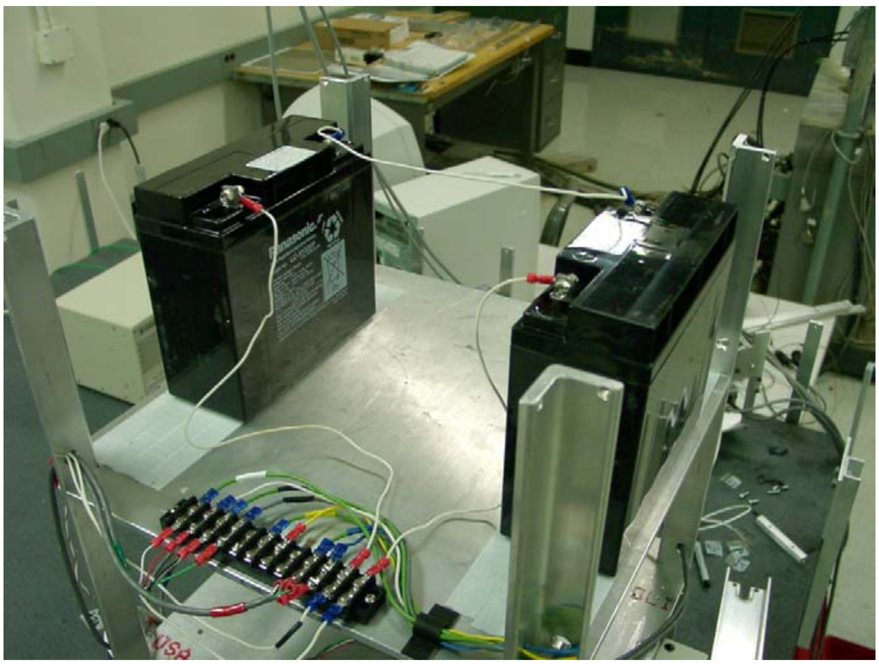

Figure 10 NPADS Battery Layout

Power to all NPADS systems, with the exception of the computer, is controlled by a single toggle switch located on the simulators left side under the second shelf. Battery power to the computer is controlled by a separate switch, located on the first shelf, to enable switching between off-board AC power and battery power. Each of the +18, +12, +6 and ±5 volts are provided by a series of dc-dc converters, also mounted on the underside of the second shelf (Figure 11). A detailed wiring diagram of the NPADS power distribution is presented in Figure 56 of Appendix A. The +6 volt supply is wired directly to the thruster system, while each of the other voltages is accessed via a barrier strip mounted near the back of the third shelf (see Figure 10). Figure 12 contains a diagram of the barrier strip power distribution.

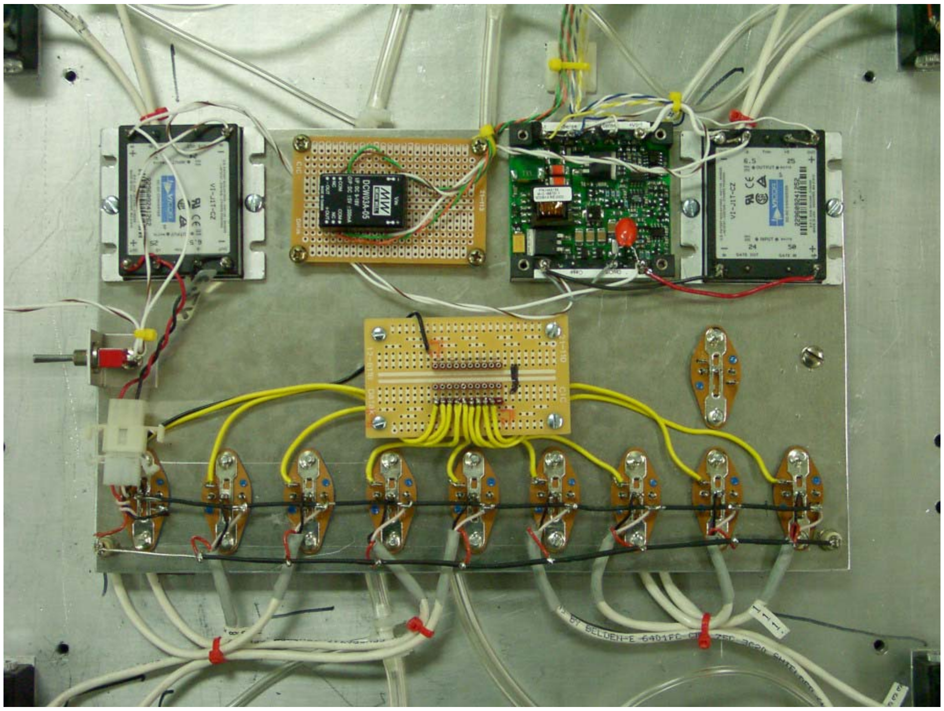

Figure 11 NPADS DC-DC Converters

Both of the NPADS batteries are mounted to the third shelf with Velcro so that they can be moved forward or aft to adjust the center of gravity and inertia mass properties of the vehicle. Table 3 contains a list of all the simulator systems and their individual power requirements.

Table 3 Simulator Component Power Requirements

Simulator Component	Voltage (vdc)	Peak Current (A)	Power Consumption (W)
Computer	24	6.25	150
Reaction Wheel	18	0.42	7.5
Thrusters	6	5	2.4 / thruster
Rate Gyro	5 and -5	<0.075	<0.8
Accelerometer	5	0.0036	0.018
CCD Camera (Star sensor)	12	0.126	1.512
CCD Camera (Docking System)	12	0.2	2.4
Wireless Ethernet	12	0.18	2.16

1	2	3	4	5	6	7	8	9	10	11	12
Grd	-5 vdc	Grd	+5 vdc	Open	Grd	+12 vdc	Open	Grd	+18 vdc	Grd	+24 vdc

Figure 12 NPADS Power Distribution Barrier Strip Diagram

E. COMPUTER SYSTEM

An onboard computer, mounted on the second shelf, controls every aspect of NPADS operation. The computer system is manufactured by National Instruments and consists of a 1000B chassis, PXI 8175 controller, PXI 6070E Multifunction I/O Card, PXI 6713 Analog Output Card and PXI 1408 Machine Vision Card (Figure 13). In addition, expansion slots are available for future robotic arm control cards. The system leverages PXI technology and a single source for fast and easy integration and synchronization of data acquisition systems. In addition, a wireless Ethernet system allows wireless data acquisition and control.

1. Chassis and Controller

The 1000B chassis uses an AC or 10-32 volt DC power supply that allows operation from the batteries for fully autonomous docking or from an external power source. In addition to the controller slot, the chassis has 7 expansion slots for the required data acquisition and control cards. The PXI 8175 controller utilizes an 866 MHz Intel Pentium III processor and has built-in Ethernet and serial ports [Ref. 3]. The system uses the Windows 2000 operating system.

2. PXI 6070E Multifunction Input/Output (I/O) Card

The PXI 6070E I/O Card is a multifunction analog and digital interface for PXI [Ref. 4]. NPADS uses the 6070E Card to control the reaction wheel and acquire rate and acceleration data. A complete description of the 6070E pin out utilization is provided in Table 11 of Appendix A.

3. PXI 6713 Analog Output Card

The PXI 6713 Analog Voltage Output Card has eight analog output channels, eight digital I/O channels and two general purpose counters for counting external pulses or clock pulses [Ref. 5]. Due to the signal noise created by the NPADS thrusters, the 6713 digital I/O channels are used to control the eight cold-gas thrusters, separating them from the rate sensor and accelerometer data on the 6070E card. In addition, three counters are used for reaction wheel RPM measurement. A complete description of the 6713 pin out utilization is provided in Table 2 of Appendix A.

4. PXI 1408 Machine Vision Card

The PXI 1408 Card is an image acquisition card that uses an 8-bit flash analog-to-digital converter to acquire an image in real time and transfer it to system memory [Ref. 6]. A black and white "star sensor" camera and color CCD docking camera provide video to the 1408 card via a standard BNC connector.

5. Wireless Ethernet

A Proxim RangeLAN2 7920 Series Ethernet adapter is used to remotely command and control NPADS. In addition, all data acquisition during testing was collected remotely for completely autonomous operation. The RangeLAN2 operates with a 2.4 GHz carrier frequency and has a 1.6 Mbps data rate.

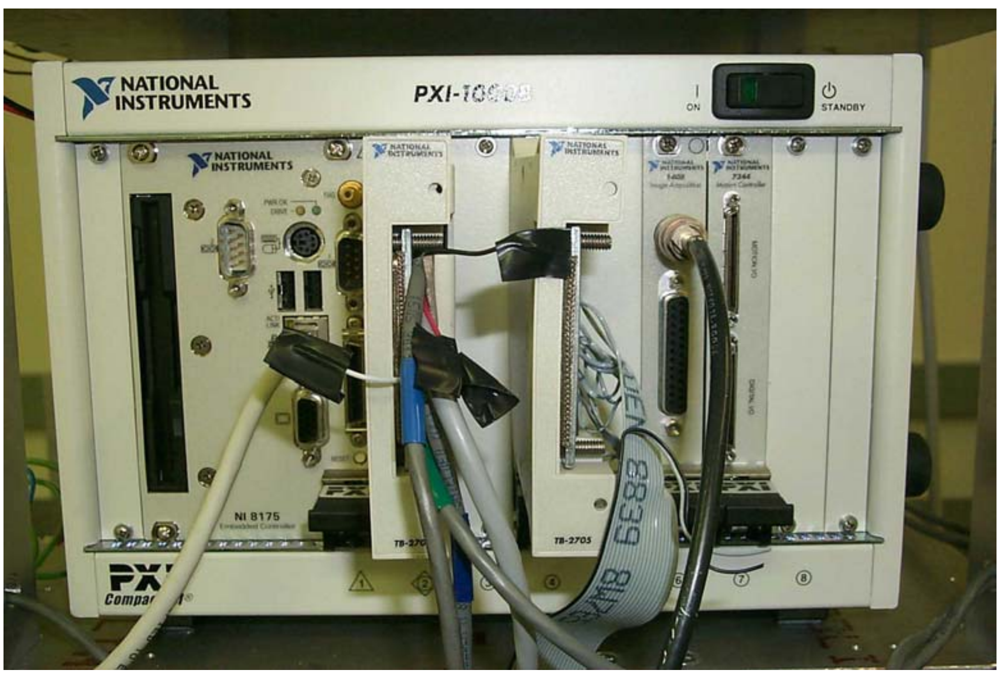

Figure 13 NPADS Computer System

F. RATE SENSOR

NPADS uses a BEI Systron Donner QRS11 Quartz Angular Rate Sensor for feeding back rotational motion. Using Microelectromechanical Systems (MEMS) technology, it measures 1.2 inches in diameter and weighs less than 60 grams (Figure 14). The rate sensor requires +5 and –5 volts dc input and provides +/- 2.5 volts dc output corresponding to +/-100 deg/sec maximum rate (25mV/deg/sec). The rate sensor wire harness design is included as Table 13 of Appendix A. The use of a MEMS technology rate sensor resulted in a tremendous savings in real estate and facilitated mounting the sensor as close to the simulator spin axis as possible, on the underside of the first shelf.

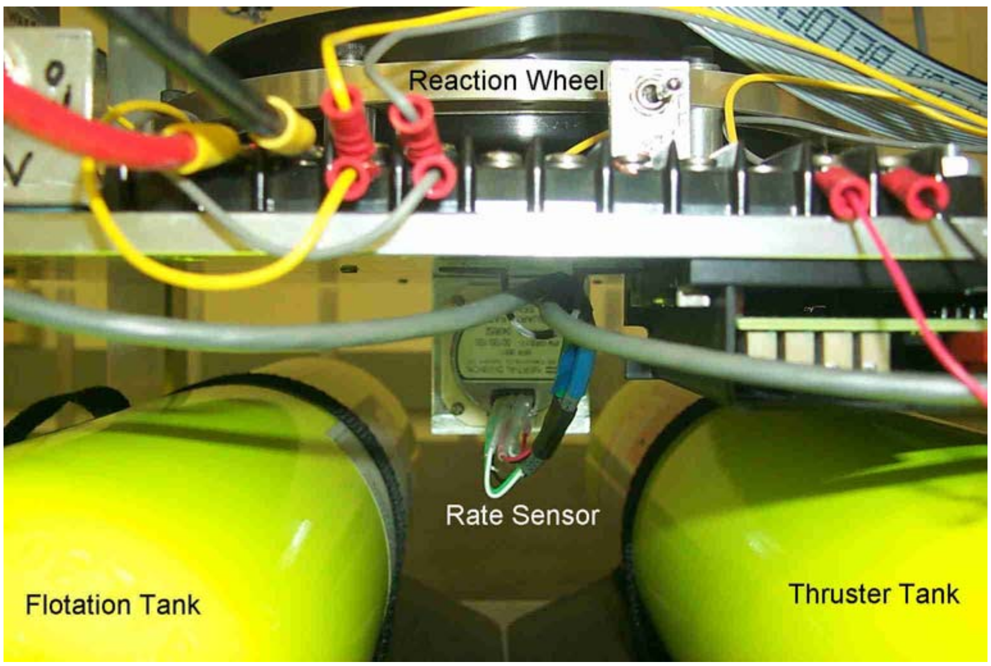

Figure 14 MEMS Angular Rate Sensor

G. PROPULSION

1. Thrusters

The NPADS cold gas thrusters are commercially available micro solenoid valves from Farmington Engineering Inc (Figure 15). Eight thrusters are mounted underneath the second shelf and are numbered 1-8 as depicted in Figure 16. A 19 cu ft scuba tank provides the “fuel” for each thruster, in the form of 150-psi air, via 1/16-in ID x 1/8-in OD polyurethane tubing. In order to produce usable thrust, a hose-fitting nozzle is attached to the exit port of each valve which results in an output thrust of 0.076 lbf (0.34 N). Each normally closed thruster is controlled via digital lines 0-7 on the computer PXI

6713 card and requires 6 volts dc to operate. The thruster control circuitry, located under the second shelf, is depicted in Figure 57 of Appendix A.

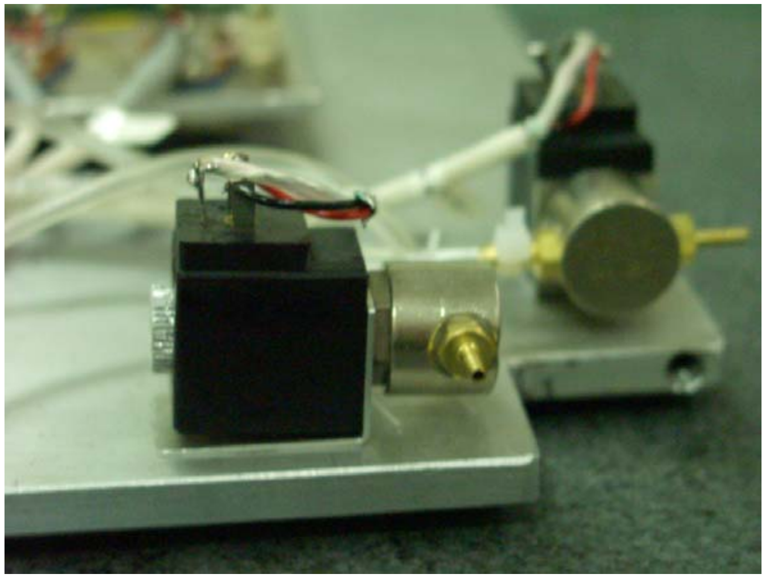

Figure 15   NPADS Thruster

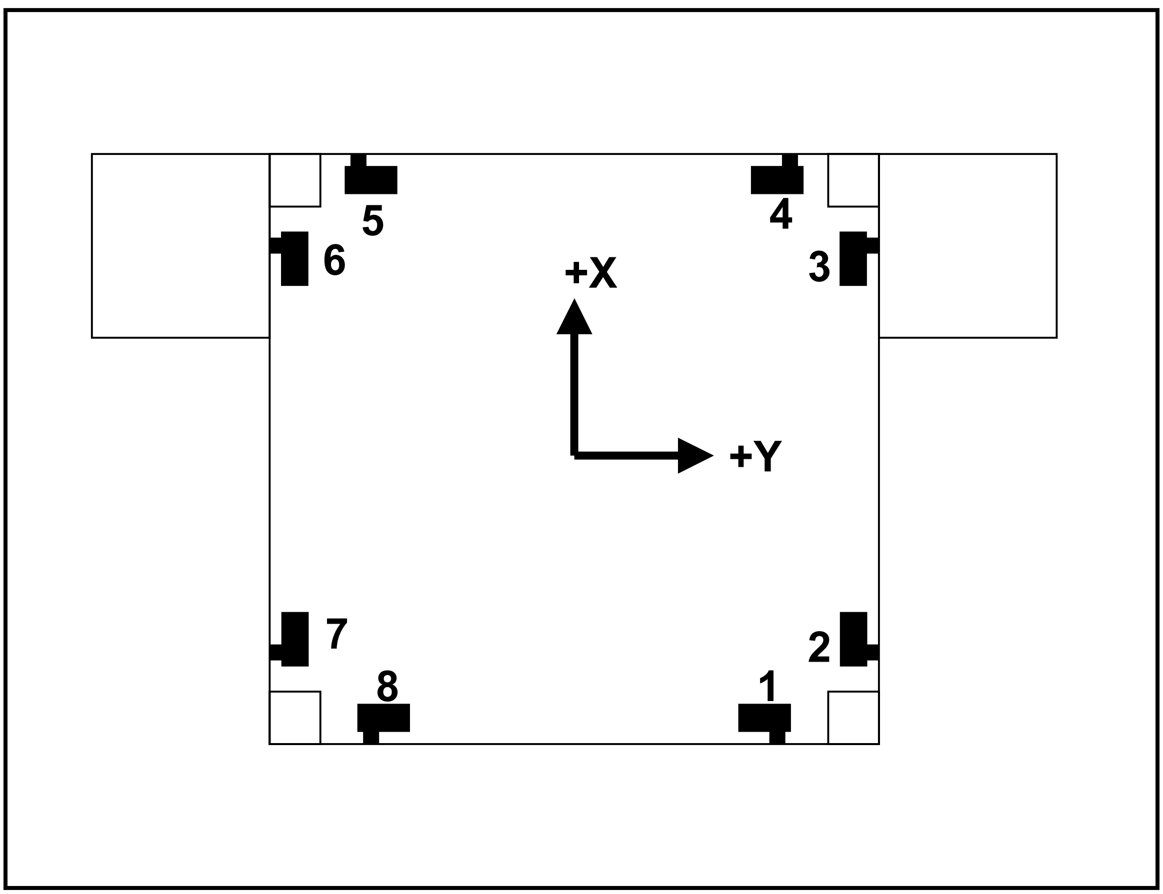

Figure 16   NPADS Thrusters

2. Reaction Wheel

A Ball Aerospace reaction wheel is located in the center of the first shelf as depicted in Figure 17.

Figure 17 NPADS Reaction Wheel

The NPADS reaction wheel is powered by 18 vdc and has a total angular momentum of 2.5 N-m-s at 2350 rpm. An analog torque command signal, having an amplitude of ±2 vdc, is sent to the reaction wheel via the 6070E Multifunction I/O card resulting in a torque of ±8 oz-in respectively. The wheel utilizes three hall sensors, connected to the 6713 analog data acquisition card, for rpm measurement with a scale factor of 15 rpm/Hz. A switching shunt regulator, mounted next to the reaction wheel on the first shelf, was incorporated in the circuitry to prevent damage during motor reversal and deceleration. The reaction wheel shunt wiring diagram, harness design and 6070E card pin out are included in Appendix A. While the reaction wheel is completely operational, it is only being used for manual attitude control at this time.

WARNING

Care must be taken not to command a torque greater than ±8 oz-in (±2 vdc).
Damage to the reaction wheel may result.

H. VISION SYSTEM

1. Black and White CCD Camera (Star Sensor)

A Provideo CVC-320WP CCD camera is mounted on the forth shelf and is used as a “star sensor” to determine the NPADS vehicle position on an air bearing table. The camera stands 5-1/4 in. tall with a 1/3 in. Sony B/W CCD fixed focus image sensor (Figure 18). The “star sensor” is pointed at the ceiling above the table and is used to locate and determine the position, within 1/10 of an inch, of a black reference circle. A white line, painted on the body of the camera, is used to align the camera with the vehicle X and Y axis. The camera is powered by 12 vdc and has a shutter speed of 100 Hz.

Figure 18 “Star Sensor” Camera

2. Color CCD Docking Camera

A Sanyo VCC-3972 color CCD camera is mounted on the top of NPADS facing forward as depicted in Figure 19. The camera uses a Tokina TVR 3314 verifocal lens with auto iris and has an adjustable electronic shutter with speeds from 60Hz to 10,000Hz. During initial testing of the camera, the black and white mode was used due to the slow computer picture capture while using color modes. The camera is not used for NPADS control at this time but will eventually be used for locating and tracking a docking target. The camera is powered by 12 vdc from the power barrier strip located on the third shelf.

Figure 19 NPADS Docking Camera

I. MASS PROPERTIES

Each component of the NPADS vehicle was carefully weighed prior to installation. Following the final build-up and just prior to testing, the entire vehicle was weighed to ensure an accurate mass analysis. During design, an effort was made to keep the center of mass near the geometric center of the vehicle and to make the vehicle as symmetrical as possible to minimize the products of inertia. The vehicle axis system was set up with the origin at the geometric center of the vehicle base for all mass property calculations as depicted in Figure 20. Detailed mass properties calculations are presented in Table 15 of Appendix B. The center of mass was determined to be approximately -0.64 in., -0.10 in., -15.08 in. in the X, Y and Z directions respectively.

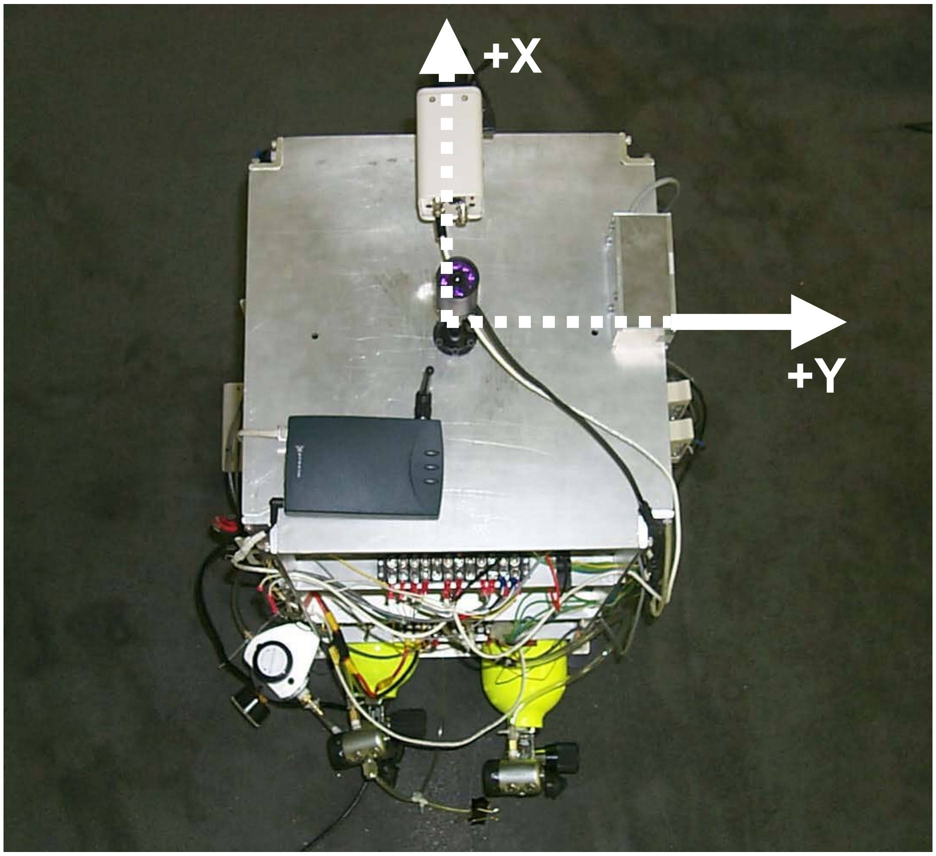

Figure 20 NPADS Axis System

A summary of the vehicle moments of inertia is provided in Table 4.

Table 4 NPADS Mass Properties

Property	Value
Mass	142 lbm
Center of Mass (x)	-0.64 in
Center of Mass (y)	-0.10 in
Center of Mass (z)	-15.08 in
Ixx	45.575 ft-lb-s^2
Iyy	44.093 ft-lb-s^2
Izz	17.402 ft-lb-s^2

(1) All cross-products of Inertia were determined to be less than 2.2 ft-lb-s^2.

THIS PAGE INTENTIONALLY LEFT BLANK

III. SUPPORT SYSTEMS

NPADS was designed so that it can be easily maintained and will require minimal down time throughout the life of the project. With this in mind, one of the primary goals was to minimize any dependency on outside sources for routine maintenance and servicing. This goal was achieved primarily through the use of commercially available components and a completely independent design. The only consumables required to operate NPADS are electricity to charge the batteries and compressed air for flotation and thruster operation. This not only simplifies the required maintenance but also minimizes the funding required for future research. This chapter describes each of the NPADS support systems and the critical role they play in supporting the NPADS vehicle.

A. GRANITE TABLE

A 6x8 ft Mojave granite table provides the required air bearing surface for NPADS operation (Figure 21). Due to the size of the air gap between the NPADS air pads and the table (20 micron), the surface of the table must be kept clean. Following a general cleaning of the table with a vacuum cleaner, the table was dusted using a very fine fiber brush and coated with CRC Heavy Duty Silicon Spray. An aluminum fence structure was constructed and attached to the sides of the table to prevent NPADS from leaving the table during testing. In order to minimize external disturbances, the table was leveled using four automobile jacks, one under each corner of the table. While the existing granite table provides the perfect platform for our initial research, a larger air-bearing surface will be required for future testing of some docking applications.

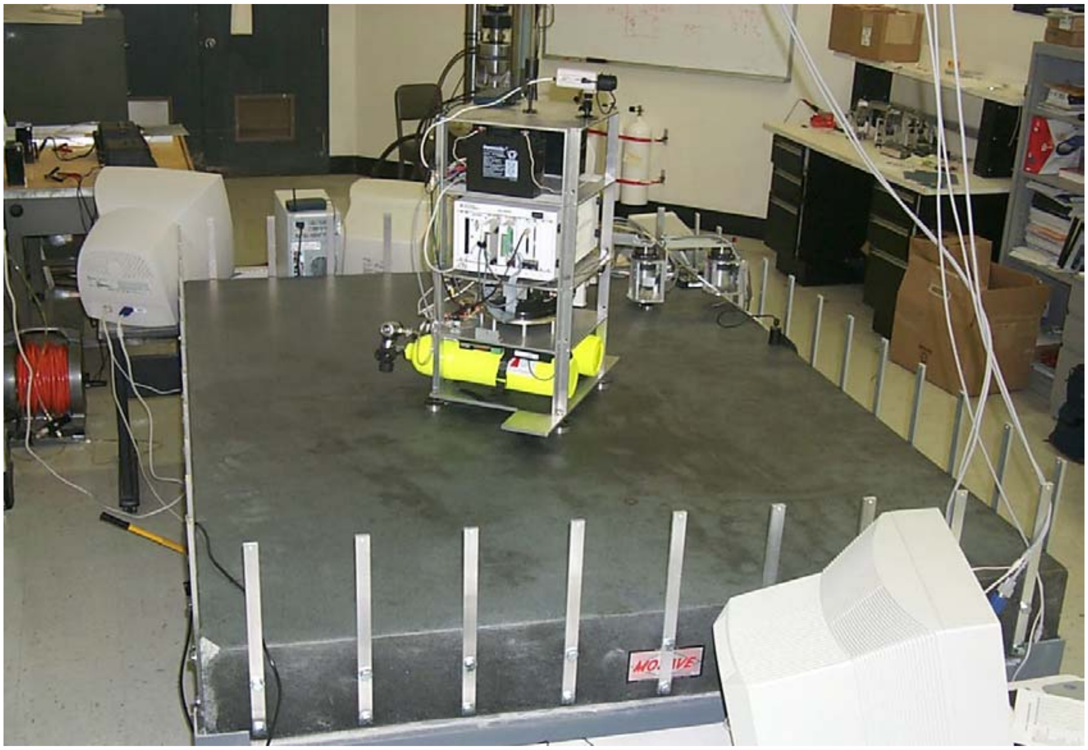

Figure 21   NPADS Granite Table

B. FLOTATION AND PROPULSION RECHARGING SYSTEM

The two 3000 psi, 19 cu ft scuba tanks that provide the source of air for flotation and propulsion are recharged in the lab from three 3500 psi, 120 cu ft scuba tanks (Figure 22). The tanks are connected for recharge using standard dive equipment fittings. During testing, each of the three re-supply tanks provided three propulsion tank refills and 3-4 flotation tank refills before it had to be serviced. The re-supply tanks can be refilled / serviced at any dive shop. In order to provide a reasonable operating time, the propulsion tank had to be filled to at least 2500 psi while the flotation tank could be filled to 2000 psi. Table 5 lists the basic steps required in re-filling the NPADS tanks.

Figure 22 NPADS Tank Recharge Station

Table 5 NPADS Air Tank Filling Procedures

1. Ensure all tanks OFF and all fittings are clean.
2. Ensure filler valve and line bleed valve closed on filling adapter.
3. Check O-ring on filling adapter.
4. Connect filling adapter to supply tank.
5. Connect tank to be filled.
6. Open supply tank valve. (NOT filling adapter valve yet)
7. Open tank to be filled.
8. Crack open the filling adapter valve and begin to fill tank slowly.
   (DO NOT EXCEED 3000 psi)
9. Close filling adapter valve and let sit 3-5 minutes.
10. Crack open the filling adapter valve to top off the tank.
    (DO NOT EXCEED 3000 psi)
11. Close the filling adapter valve.
12. Close the tank being filled.
13. Close the source tank valve.
14. Open the filling adapter valve to bleed pressure.
15. Open the bleed valve until pressure reads zero on filling adapter.
16. Close all valves and the bleed air valve.
17. Disconnect filling adapter and check O-ring.

C. COMPRESSOR

Flotation of the NPADS vehicle can be accomplished using a compressor and umbilical connection. The NPADS compressor system consists of a Puma 125 psi compressor which is connected to the vehicle via a 1/4in ID x 3/8in OD umbilical. During initial testing, the compressor system was used to verify proper component operation, however the umbilical caused too much of a disturbance for meaningful data acquisition. In addition, the compressor air filter could not remove all of the oil in the compressed air resulting in contamination of the flotation system. In the event the compressor system is used in the future, a better air filter will be required.

D. ELECTRICAL RECHARGING

The NPADS batteries can be recharged on or off the vehicle using two DieHard 10/2/60 Amp battery chargers (Figure 23). The chargers plug into a standard 120 vac receptacle and will automatically terminate charging once the battery is fully charged. In order to prolong the life of the battery, the slower 2 amp charge rate is used. A total of four batteries are available so that two can be charged while the simulator is being operated. The average charge time is approximately three hours.

Figure 23 NPADS Electrical Recharging

E. OPERATOR CONTROL AND DATA ACQUISITION COMPUTER

NPADS is remotely operated from a control and data acquisition computer via wireless Ethernet (Figure 24). Both the NPADS computer and the remote computer run LabView and exchange information using the National Instruments Data Socket Server, a TCP/IP manager that links data via wireless Ethernet. Data obtained from NPADS is stored in a text file on the remote computer, freeing up memory on the on-board computer. Prior to remote control, the NPADS computer must establish a network connection with the remote computer. The mouse/keyboard and monitor cables are then disconnected from NPADS and the remote computer has control. For a detailed description of the control and data acquisition computer programming, see chapter IV.

Figure 24 NPADS Control / Data Acquisition Computer

F. NPADS WORKSTATION

The NPADS on-board computer is programmed and initialized for operation using a monitor, mouse and keyboard that can be disconnected prior to commanding the vehicle. The NPADS workstation (Figure 25) includes cables that hang from the ceiling so that the workstation can be plugged into the vehicle anywhere on the granite table.

Figure 25 NPADS Workstation

IV. NPADS CONTROL SYSTEM

The NPADS control system was developed in several logical stages. During the first stage, Matlab Simulink was used to create a theoretical model of the NPADS thruster control scheme using the basic mass properties and thruster configuration. At the same time, a manual control algorithm was developed in Labview, the programming medium used to control the actual NPADS vehicle, to test the basic functionality of the NPADS components. Based on the results obtained during simulation and manual control, the first Labview autonomous control algorithm was developed.

This initial autonomous control algorithm, a basic PD control scheme, is the first step towards the implementation of the desired neural network control. Because the target vehicle is still being developed, no specific docking applications have been investigated thus far using the existing PD control algorithm. Once the target vehicle is available and the desired visual target designed, the color CCD docking camera and reaction wheel are fully functional and will be ready for integration into the control algorithm.

A. THRUSTER CONTROL MODEL

A basic PD control algorithm was created using Matlab Simulink to investigate the basics of controlling a bang-bang type thruster and simulate the vehicle response. As part of the simulation development, the thrusters were tested and determined to produce a force of 0.35N (0.078 lbf). The NPADS thruster and axis orientation are depicted in Figure 26. The simulation was developed in two parts; torque control and translational control.

1. Torque Control

A moment arm of 7 in (0.58 ft) was assumed for the torque control simulation. For positive torque about the z-axis, thrusters 1, 3, 5, and 7 are fired and for negative torque, thrusters 2, 4, 6, and 8 are fired. The torque impulse bit is $I = F \cdot \Delta t \cdot \Delta x$, where Δt is the amount of time the thruster is on. Thruster firing is a non-linear function due to the fact that the thruster is either on or off and the amount of torque imparted to the vehicle is dependent on the thruster on time. Converting the required torque into a thruster on-off scheme is therefore achieved through the use of pulse-width-modulation (PWM) [Ref. 7 and 8].

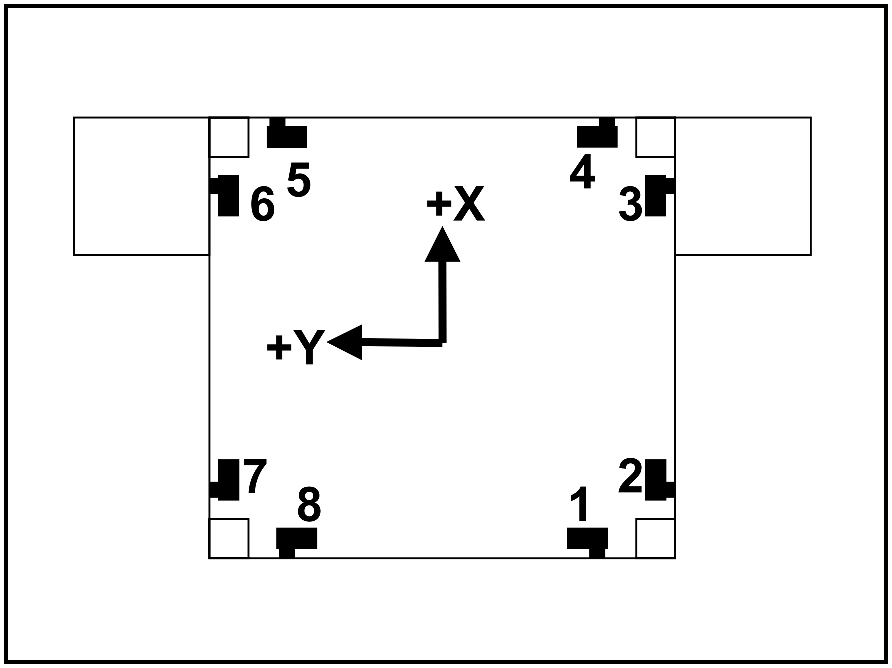

Figure 26   NPADS Thruster Arrangement

With a linear actuator, like a reaction wheel, we could apply the desired torques directly. The equation of motion for the rigid body spacecraft would then be $J_Z \cdot \ddot{\theta} = \tau$. Using a PD control input of the form $\tau = K_{P_Z} \cdot \theta + K_{d_Z} \cdot \dot{\theta}$, we initially choose K_{P_Z} and K_{d_Z} such that it meets the characteristics of a critically damped system, that is, $\omega_{n_Z} = 1$ and $\zeta = 1$. The PD control gains are then given by $K_{P_Z} = \omega_n^{\ 2} \cdot J_Z$ and $K_{d_Z} = \left(2\zeta\sqrt{J_Z / K_{P_Z}}\right) K_{P_Z}$ from which the basic PD simulation can be formed as depicted in Figure 27.

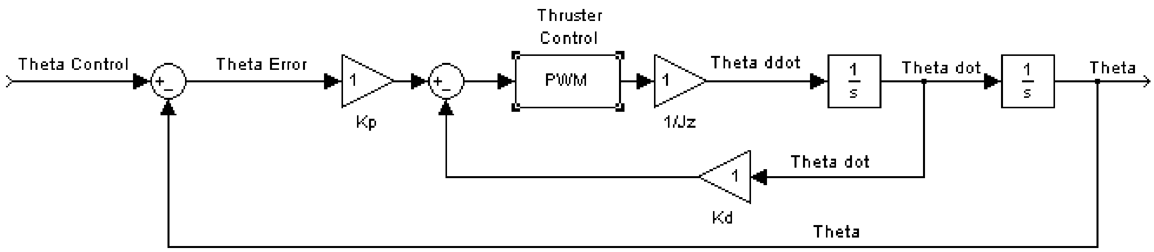

Figure 27 Basic PD Theta Control

To implement thruster control, the PWM scheme is inserted as depicted in the figure above. The desired torque remains the same as if we were using a reaction wheel. The output of the PWM system is an on/off signal that varies in length (time) proportional to the input signal (τ). The output is then a 0 or 1 sent to each of the thrusters to be controlled. The torque from the thrusters is then given by $\tau_Z = F \cdot \Delta x \cdot (T1 + T3 + T5 + T7)$, where T# is the time that a particular thruster is on, in this case for positive torque. For the four identical thrusters, all equally spaced, $T_{ON} = \tau_Z / (4 \cdot F \cdot \Delta x)$.

If we could control the time in a continuous manner, then any value of T_{ON} would directly come from the above equation. Thrusters, however, have a limited on-off cycling time and the actual control system on a spacecraft is discrete. The sampling frequency of the control system is usually fixed, requiring the use of a fixed time step integration scheme in the Simulink simulation. In the NPADS simulation, the ODE4 (Runge-kutta) with a fixed time step of 0.005 seconds was used.

The Simulink model is a continuous, not discrete, simulation. Therefore, a PWM system had to be developed to work in this framework. The simplest analog form of generating fixed frequency PWM is by comparison with a linear slope waveform like a saw tooth (Figure 28). As depicted in the figure, the output signal goes high (1) when the sine wave goes above the saw tooth (a and b) and goes low when the sin wave drops below the saw tooth (a' and b').

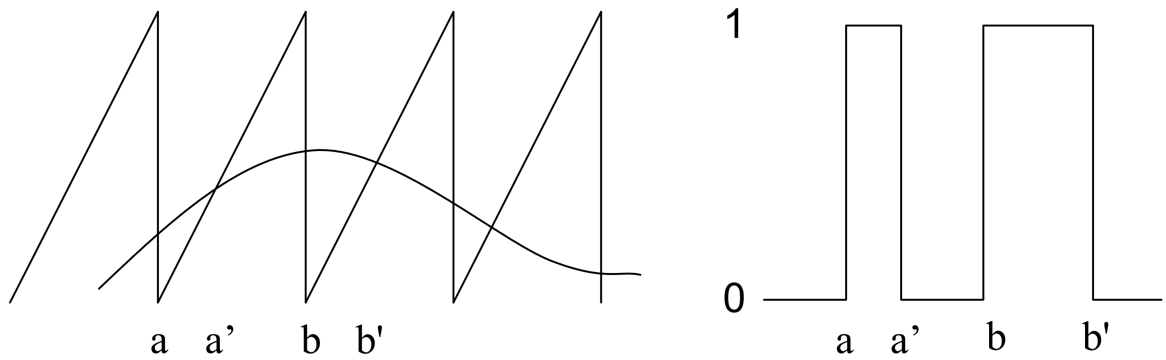

Figure 28 PWM Saw Tooth Waveform

This is implemented using a comparator whose output voltage goes to logic high (1) when one input is greater than the other (Figure 29).

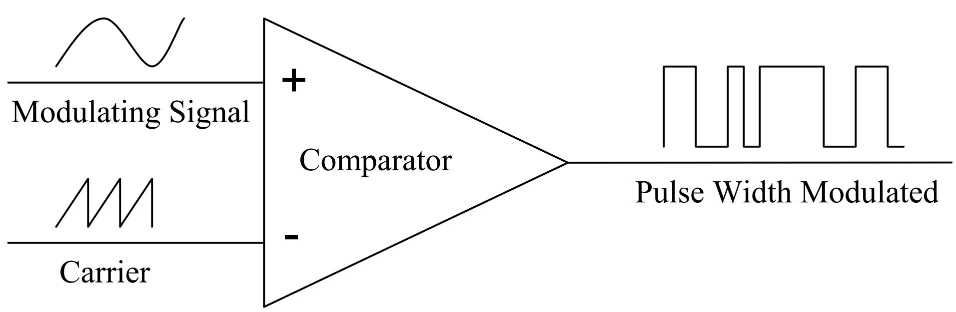

Figure 29 PWM Comparator

The amplitude and frequency of the carrier are chosen based on some general knowledge of the modulated signal. For the NPADS control simulation, an amplitude of 3 and frequency of 2 Hz were selected. A dc offset (lifting of the saw tooth) is incorporated to prevent chatter and excessive thruster firings around zero. The above scheme is demonstrated in the NPADS control simulation.

2. Translation Control

Axial translation in the X and Y direction, as depicted in Figure 26, was incorporated following much the same design thought process. The translational equation of motion is given by $F_X = ma_X$ in which F_X is controlled. Again a PD control scheme was used as depicted in Figure 30. The required thrusters for translation in the X and Y directions are given in Table 6. The PWM block is the same for translational control.

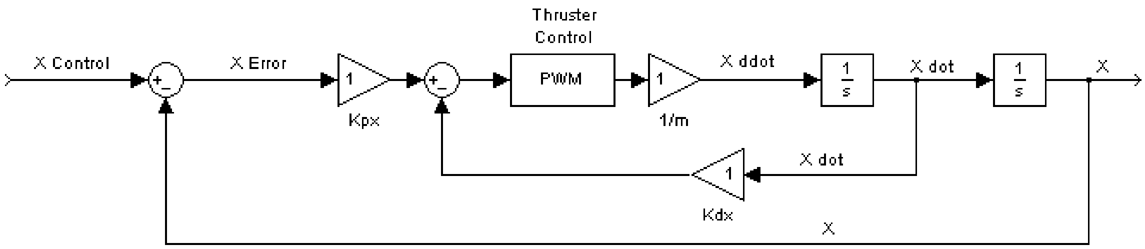

Figure 30 Basic PD X Control

Table 6 Translation Thruster Firing

Translation Direction	Thrusters Required
+X	1 and 8
-X	4 and 5
+Y	2 and 3
-Y	6 and 7

3. NPADS Simulink Control Simulation Code

The simulation was constructed in several layers. The outer layer (Figure 31) is the user interface and simulation results. The user commands a desired X, Y and theta (rotation), the results of which are then displayed on separate X, Y and theta graphs.

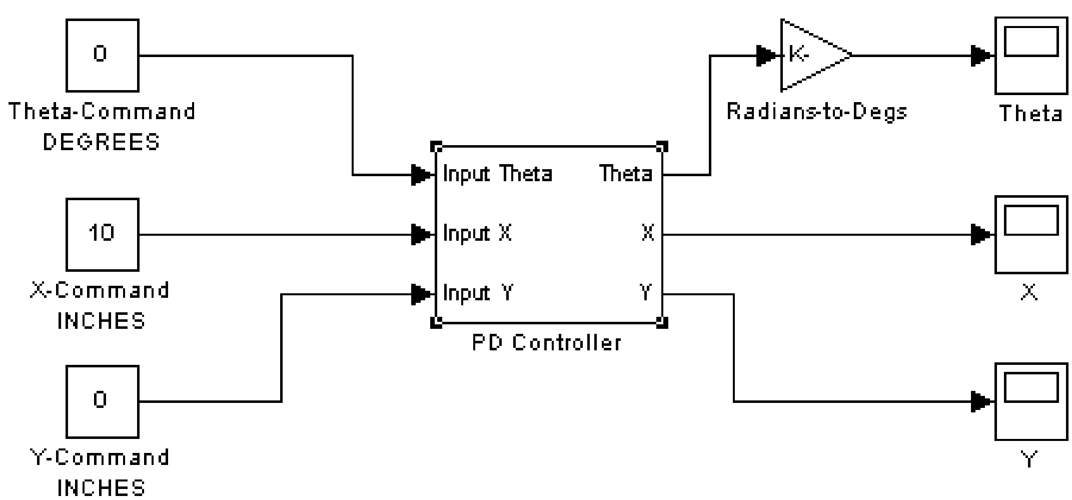

Figure 31 NPADS Simulation User Interface

The heart of the simulation is a basic PD controller for each of the three degrees of freedom, X, Y and theta (Figure 32).

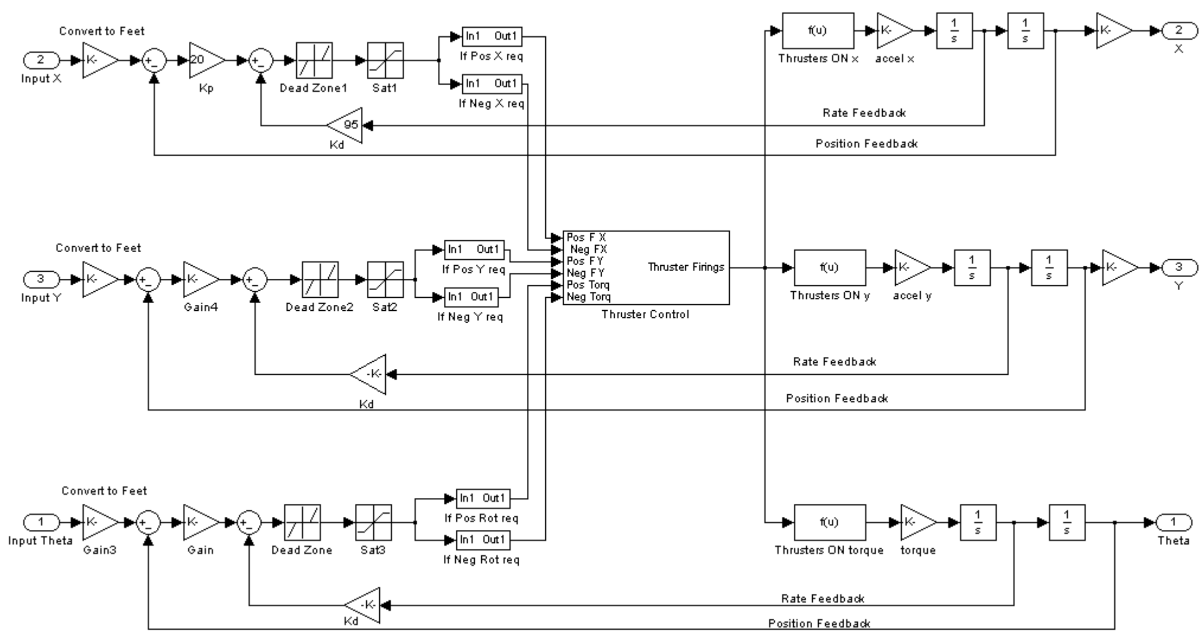

Figure 32 NPADS Simulation PD Controller

The thruster control scheme, in the center of Figure 32, takes the required torque in each of 6 directions (±X, ±Y and ±theta) and determines which thrusters to fire to achieve the desired response (Figure 33). Within the thruster control block, each thruster is assigned a weight based on the required direction and magnitude of movement which is then pulse-width modulated as required (Figure 34).

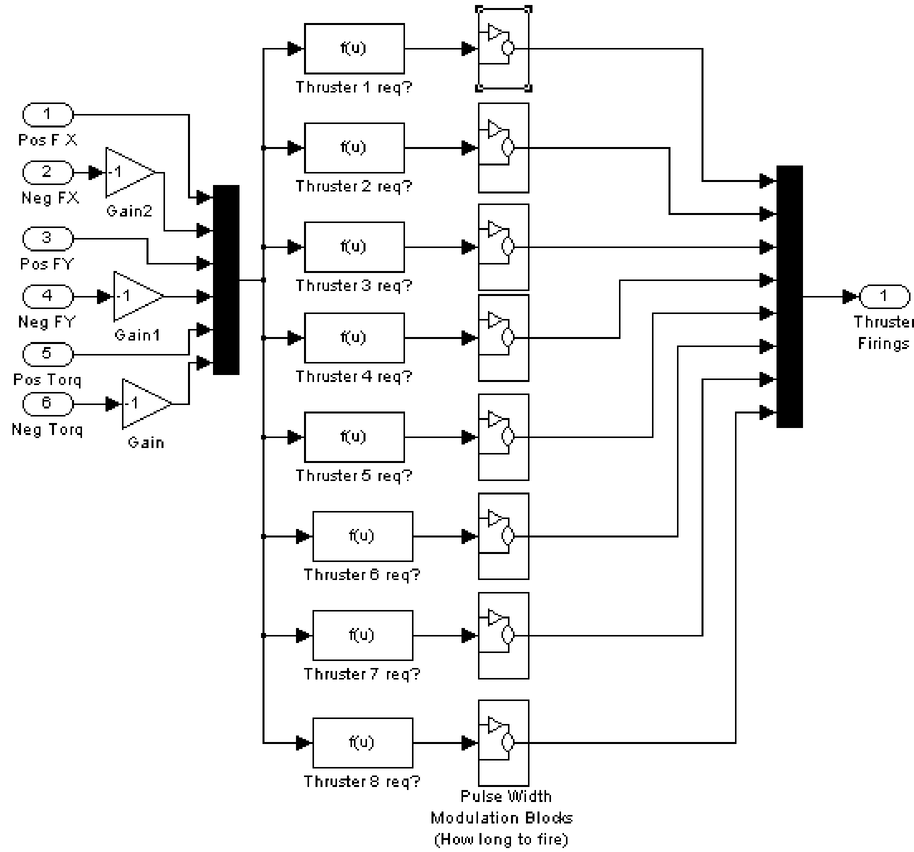

Figure 33 NPADS Simulation Thruster Control

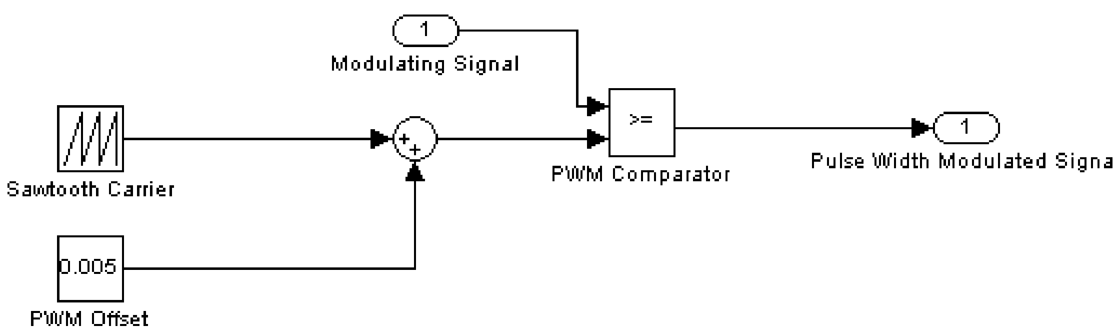

Figure 34 NPADS Simulation Pulse-Width-Modulation Block

4. NPADS Control Simulation Results

The NPADS Simulink Control Simulation provided a general idea of the expected vehicle response using a basic PD control scheme. Numerous combinations of movement in the X, Y and theta directions were tested. Table 7 lists the PD control feedback gains used in the simulation. These gains were scaled up from the calculated gains in the previous discussion to achieve the desired response.

Table 7 NPADS Control Simulation Feedback Gains

Degree of Freedom	K_P	K_d
X Translation	20	115
Y Translation	20	115
θ Rotation	7	172

The following figures demonstrate the results obtained during simulation. With this set of gains, the simulation produced the desired response and verified the PWM control scheme. Figure 35, Figure 36, and Figure 37 show the reasonably rapid response achieved in each of the Theta, X and Y degrees of freedom respectively.

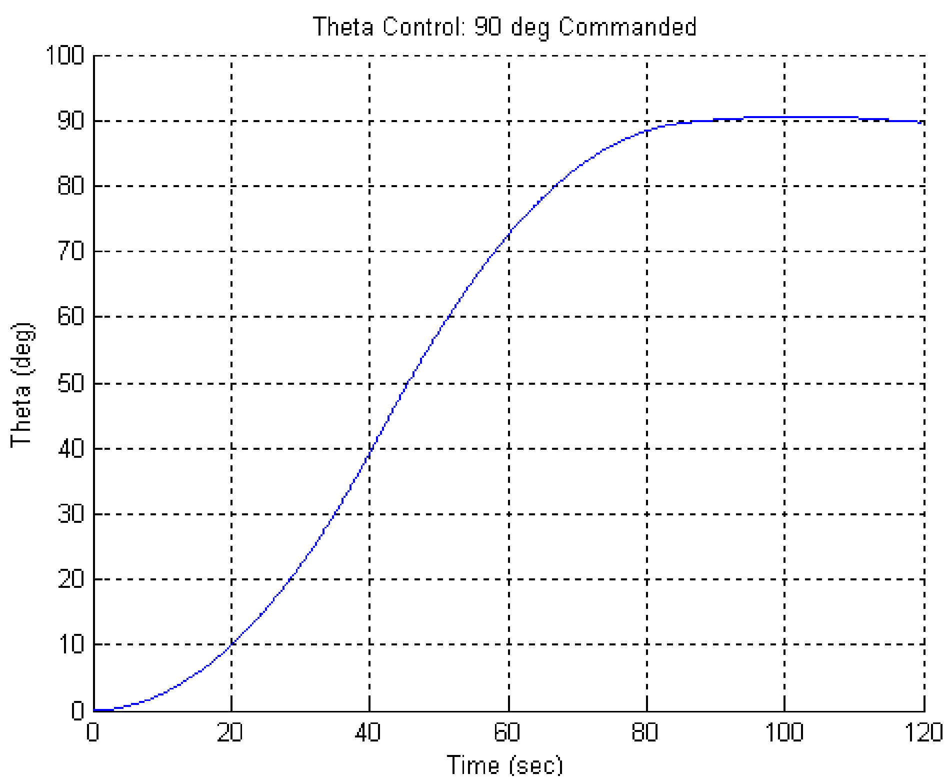

Figure 35 NPADS Simulation Theta Control Results

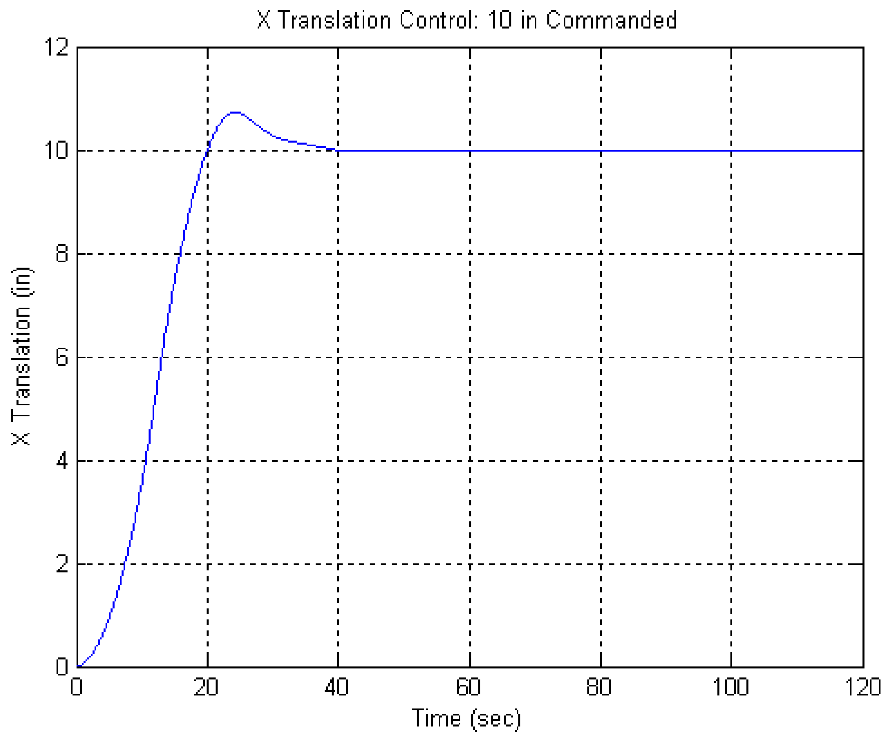

Figure 36   NPADS Simulation X Translation Control Results

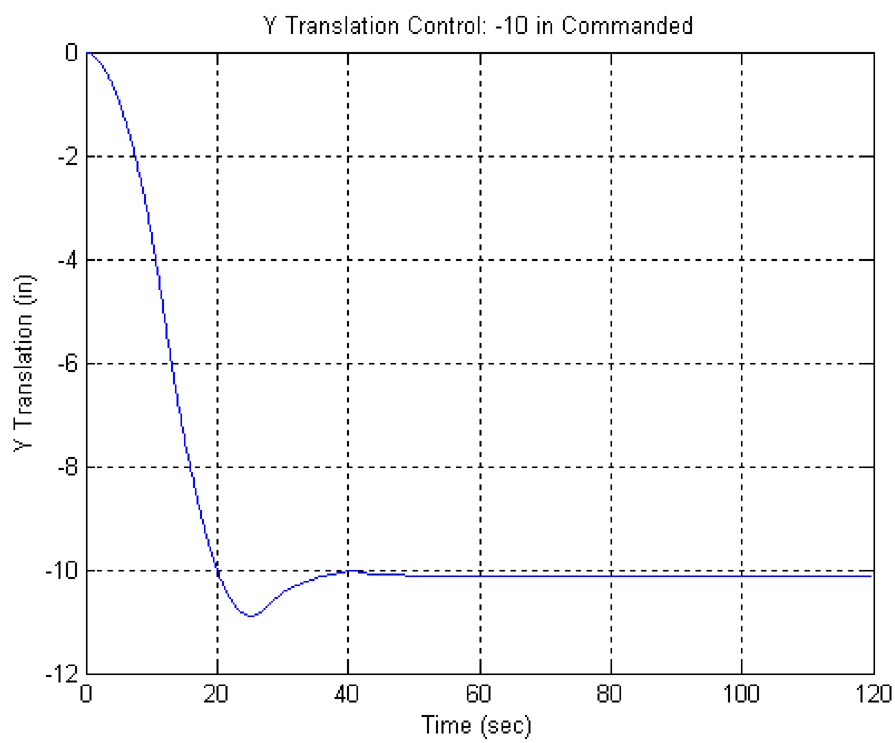

Figure 37   NPADS Simulation Y Translation Control Results

Figure 38 shows the thruster activity during the simulation that produced the above results. Most of the thruster activity is at the beginning and end of the maneuver, characteristic of a pulse-width modulated bang-bang type thruster.

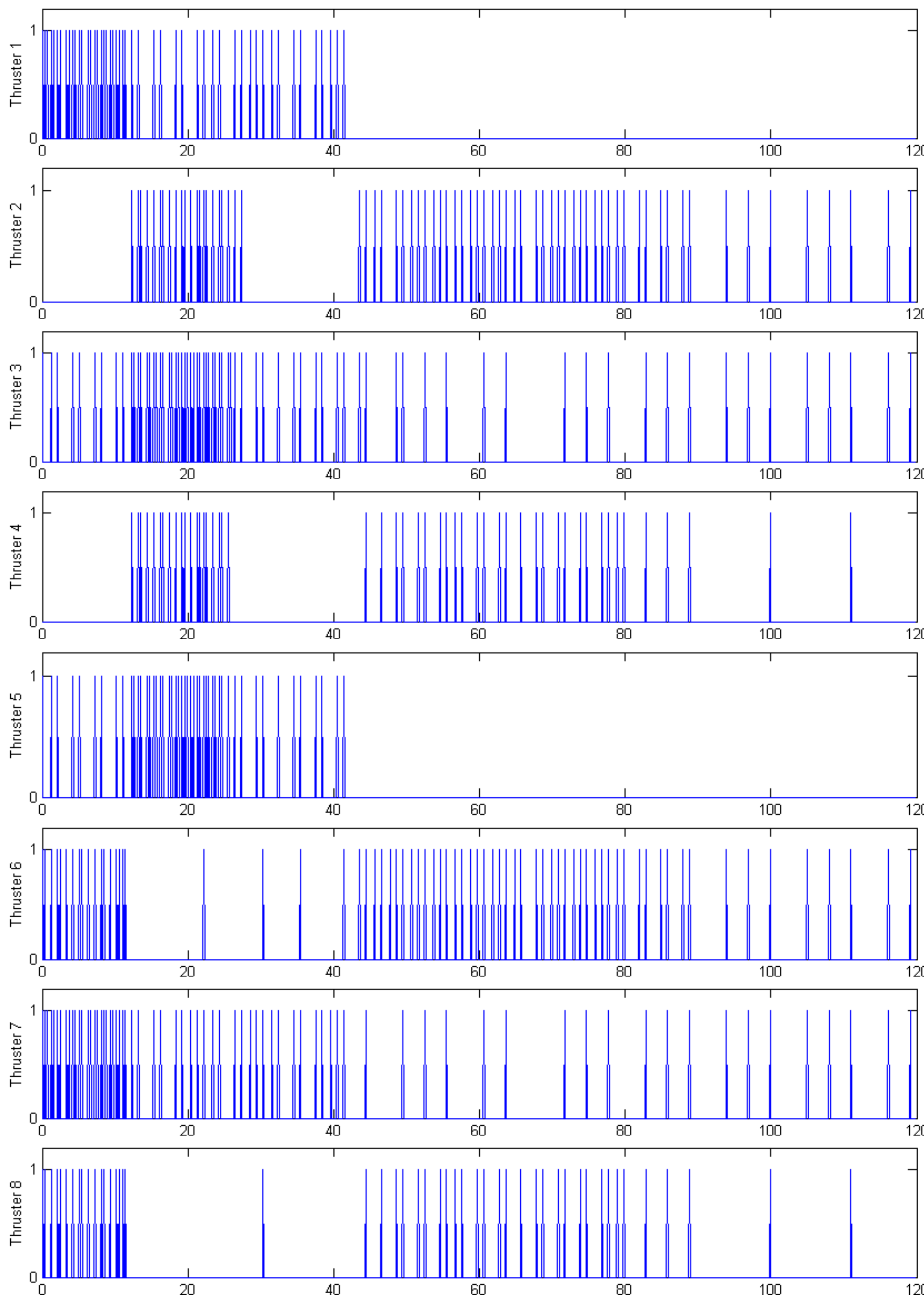

Figure 38 NPADS Simulation Thruster Activity

B. MANUAL CONTROL

Concurrently with the simulation phase of the design, a manual control program was developed to test the basic functionality of the NPADS components and become familiar with the LabView programming environment.

1. LabView

LabView is a graphical programming language specifically designed to work with a PXI computer, like the one used on the NPADS vehicle. Because the NPADS computer and control software share a common vendor, National Instruments, many of the common interface difficulties were avoided. All of the data acquisition and vision cards used were plug-and-play using LabView built-in functions. This was an extremely important design goal and will allow for rapid configuration and programming changes to the NPADS vehicle in the future. In addition, LabView provides the ability to create a user friendly graphical interface while simultaneously writing the manual and autonomous control code.

2. Manual Control Algorithm

The NPADS Manual Control Panel allows a user to manually control the eight NPADS thrusters and reaction wheel (Figure 39).

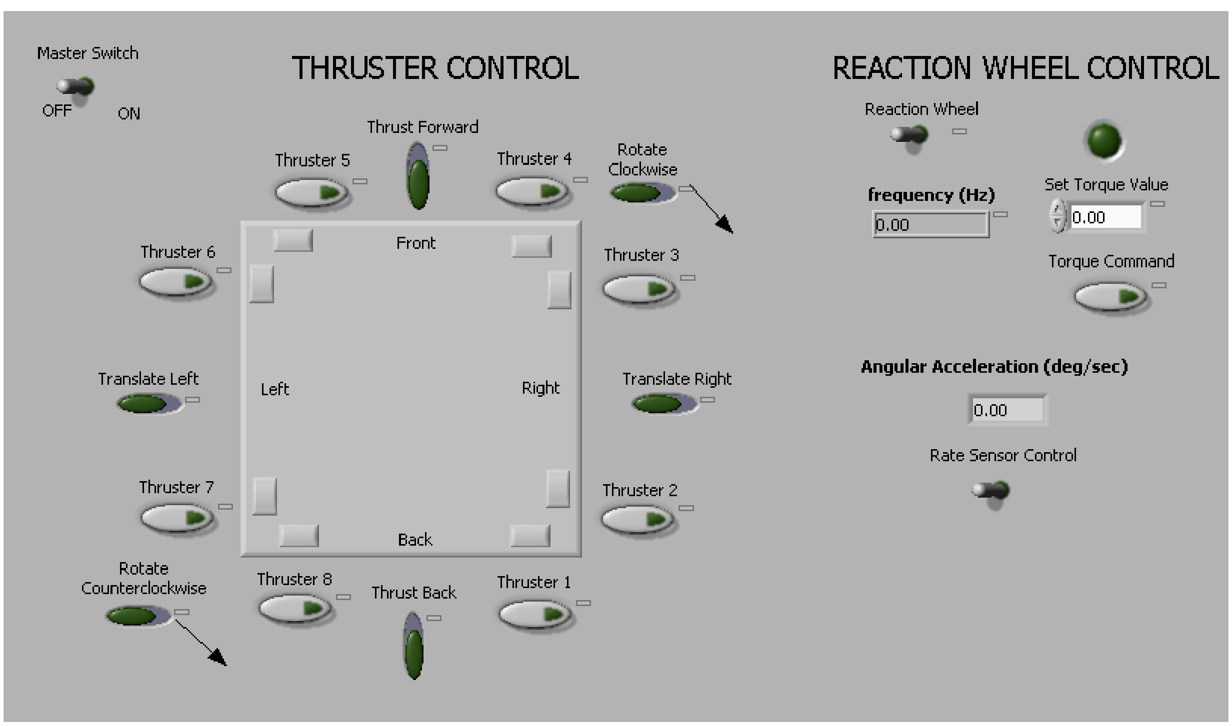

Figure 39 NPADS Manual Control Panel

The user can control each of the eight thrusters individually, two at a time for translation, or four at a time for rotation by depressing and holding the appropriate button on the control panel. In addition, the reaction wheel can be controlled by typing in the desired torque value (±8 oz-in) and depressing and holding the torque command button. The angular rate sensor is controlled on or off by a single toggle switch on the control panel and displays the current angular acceleration of the vehicle. The manual control program is run from the remote data acquisition computer and commands are sent to the NPADS vehicle via the wireless Ethernet adapter and the National Instruments Data Socket Server. For a more detailed description of the NPADS manual control algorithm and the actual code, see Appendix C.

C. AUTONOMOUS CONTROL

The goal of the NPADS research is to create a fully autonomous fuzzy logic controller for spacecraft capture and docking. The first step in achieving this goal was the creation of a simple proportional-derivative (PD) control scheme to verify the simulation and observe some of the vehicle dynamics.

1. Autonomous Control Algorithm

The NPADS PD control algorithm was designed much like the Matlab Simulink control simulation code. The user provides a desired location on the NPADS table using the Autonomous Control Panel (Figure 40). Each of the three NPADS degrees of freedom is controlled through a separate PD control loop, as depicted in Figure 41. The NPADS vision system provides proportional X and Y location feedback to the built-in LabView PID control subroutine for translation while the MEMS Rate Sensor provides rotation feedback via a LabView integration block. Translational rates and angular acceleration are derived within the PID subroutine for derivative feedback. While the LabView PID subroutine does include integral feedback capability, it is not being used. The LabView PID control subroutine output is then sent to a PWM subroutine for thruster control, much like the Simulink simulation. For a more detailed description of the autonomous control algorithm and the actual code, see Appendix D.

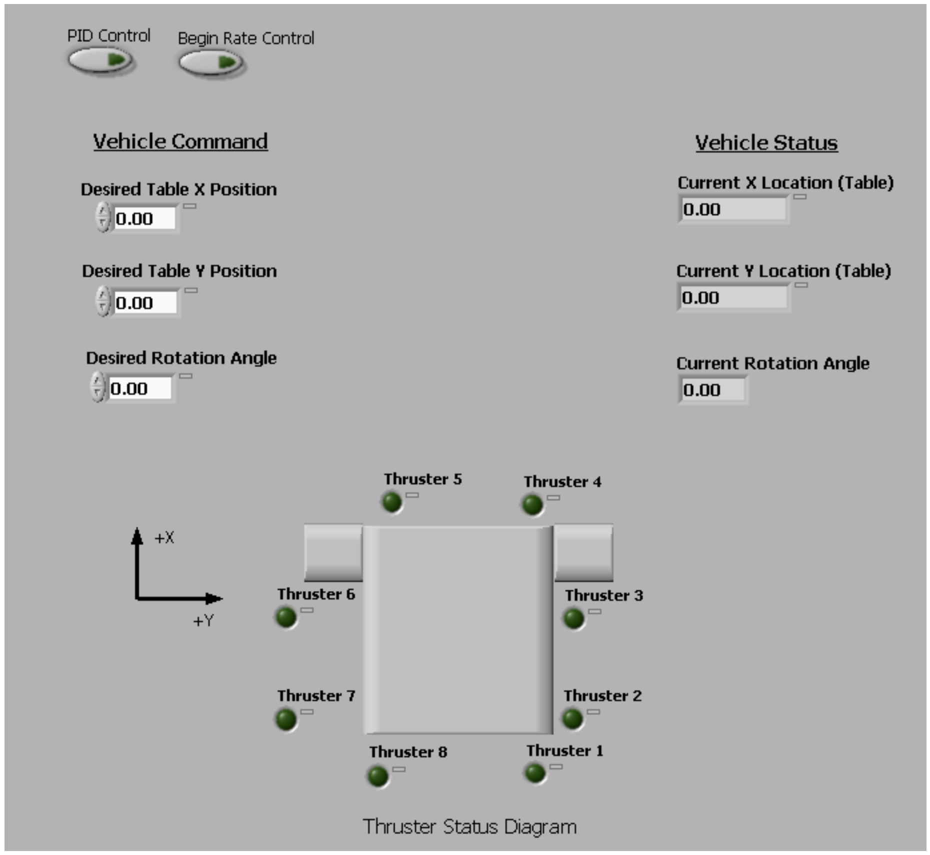

Figure 40 NPADS Autonomous Control Panel

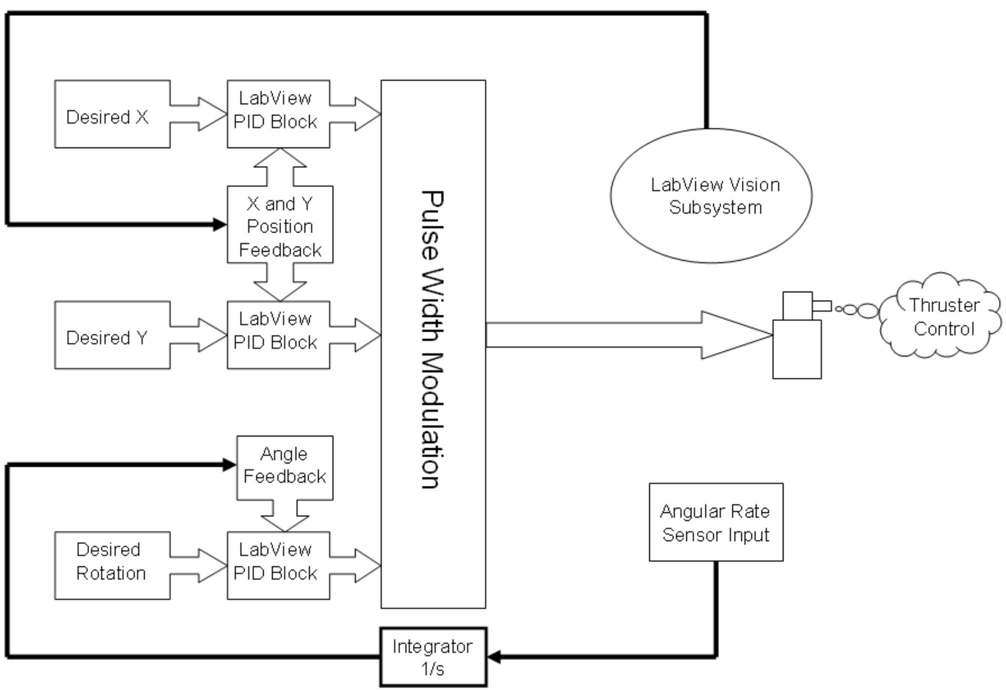

Figure 41 NPADS Autonomous Control Diagram

THIS PAGE INTENTIONALLY LEFT BLANK

V. NPADS OPERATION AND PERFORMANCE

This chapter discusses the basic operating procedures for the NPADS vehicle and the achieved performance. In the first section, power-up and power-down procedures are presented along with some routine maintenance considerations. The second part of the chapter is dedicated to the system test results and general performance characteristics.

A. NPADS OPERATION

The NPADS vehicle is operated in three phases; pre-flight, flight and post-flight. The pre-flight phase prepares the vehicle for flight and helps to identify any maintenance required. Once the pre-flight is complete, the vehicle is in the flight phase and is controlled through user inputs to the remote Control and Data Acquisition Computer. In the manual control mode, this is accomplished through user mouse commands to control individual thrusters and the reaction wheel. In autonomous control mode, the user simply enters a desired table X and Y position and the desired vehicle rotation angle with respect to the table axis system.

1. NPADS Pre-flight

The NPADS pre-flight consists of a logical sequence of tasks to boot the NPADS control computer and prepare the vehicle for flight. In addition, it includes a general inspection of the vehicle to identify required replenishment of consumables and maintenance before it effects vehicle operation. Table 8 lists the basic steps required to prepare the NPADS vehicle for flight.

The importance of a clean surface on which to operate can not be over emphasized. The NPADS granite table must be kept as clean as possible to prevent interference with the vehicle air pads. Prior to polishing the table with a Silicon spray, a very fine bristle brush was used to remove as much dust and debris as possible. This procedure was accomplished approximately every other day while testing the vehicle.

The vehicle consumables, air and battery power, are checked during every pre-flight. In order to operate the vehicle as long as possible, both air tanks should be topped off prior to operation. Flotation tank pressure can be monitored using the high pressure port indicator on the tank regulator. Due to the high discharge rate, the thruster tank should be filled prior to each flight. The NPADS battery voltage can be monitored using a voltmeter on the right side of the computer. Due to the possibility of a power loss to the control computer, the batteries should be replaced when the voltage drops below 21 vdc.

Table 8 NPADS Pre-flight Checklist

Action	Notes
1. Clean Granite Table	Use fine brush and coat with Silicon Spray
2. Check general condition of wires and hoses	
3. Align NPADS body axis with table axis	Turn on flotation tank (left tank) if required
4. Center NPADS on granite table	See Chapter II for axis orientation
5. Check Tank Pressure / turn off both tanks	Ensure tanks full for longer runs
6. Check Battery Voltage (>21vdc)	Voltmeter located on right side of computer
7. Ensure mouse and monitor connected	Should be 2 umbilical lines
8. Turn ON computer	Use AC umbilical (no password required)
9. Turn ON NPADS system power switch	Located left underside second shelf
10. Load control program	Manual or Autonomous located on desktop
11. Start Data Socket Server	On NPADS computer [Start>Programs>NI>DataSocket>DataSocket Server]
12. Prepare Control / Data Acq Computer	Run control program and data socket server
13. Start NPADS control program	Ensure no rotation for bias calculation
14. Ensure all Data Socket connections green on both computers	May need to stop and restart the Data Computer control program
15. Once bias is calculated press PID Control and Begin Rate Control buttons	Thrusters may begin to fire at this point
16. Turn ON Batteries and Unplug AC umbilical	Battery switch on rear of first shelf
17. Unplug mouse and monitor umbilical lines	Ensure they will not contact the vehicle
18. Open flotation and thruster tanks	Open valves slowly
19. Control NPADS from Control / Data Acquisition Computer	

Once the general pre-flight is completed, the NPADS control computer and the remote control and data acquisition computer are prepared for flight. The NPADS control computer is booted, the desired control program loaded and the wireless network DataSocket server started. The remote control and data acquisition computer is then prepared for flight by loading and running the appropriate remote control program and starting the DataSocket server. Once the NPADS control program is run, the remote control and data acquisition computer remote control program will need to be restarted to ensure all network connections have been established. Once the desired control program is up and running with good network connectivity, the NPADS power, mouse and monitor umbilical lines are removed for fully autonomous flight operation.

2. NPADS Flight

Upon completion of the NPADS pre-flight checklist, the vehicle is ready to receive commands in the flight mode. Commands are sent to the vehicle via user input to the Remote Control and Data Acquisition Computer. During manual control, the user commands individual thrusters and combinations of thrusters using a mouse. In addition, the reaction wheel can be commanded by entering a desired torque value with the keyboard. While running in the fully autonomous mode, the user commands the vehicle by specifying a desired X and Y position on the table and a desired rotation angle. For a more detailed description of the Manual Control and Autonomous Control Algorithms, see Chapter IV.

3. NPADS Post-flight

Upon the completion of the flight, the vehicle enters the post-flight phase of operation. The post-flight checklist, depicted in Table 9, lists the series of steps required to terminate a flight and ensure the vehicle is ready for the next flight.

Table 9 NPADS Post-flight Checklist

Action	Notes
1. Turn OFF thruster air tank	Left Tank
2. Move NPADS to desired location	Ensure AC, mouse and monitor umbilical lines will reach the vehicle
3. Turn OFF flotation air tank	Right Tank
4. Plug-in computer AC umbilical	
5. Turn OFF the batteries	Battery switch on rear of first shelf
6. Plug-in the mouse and monitor umbilical lines	
7. Stop the NPADS control program	
8. Stop the Control / Data Acquisition Program	
9. Reset the Desired Values to ZERO	On Control / Data Acquisition computer
10. Turn OFF the system power switch	Located left underside second shelf
11. Exit all control programs on NPADS computer	
12. Turn OFF NPADS computer	
13. Check NPADS Battery voltage (>21vdc)	Replace batteries as required
14. Check NPADS Tank Pressure	Charge tanks as required

In order to conserve consumables, the thruster and flotation air tanks are closed and the AC power umbilical is connected as soon as possible following flight operations. Once the control programs are terminated, the user input values to the remote control and data acquisition computer are set to zero to prevent unwanted inputs to the vehicle in the event the vehicle is flown again prior to terminating the control program. Prior to completion of the post-flight checklist, all of the consumables are checked and serviced, if required, so that the vehicle is ready for the next flight.

B. NPADS PERFORMANCE

The NPADS autonomous performance was evaluated in two different phases; Initial Test and Evaluation and Final Autonomous Operation. During the Initial Test and Evaluation phase, each degree of freedom was isolated in order to determine the best combination of control gains for the PD control algorithm. Once determined, the vehicle was tested in the final configuration.

1. Initial Test and Evaluation

During the initial test and evaluation, each degree of freedom (X, Y and rotation) was isolated and tested. Based on the observed response during the test, the control gains were adjusted and the test repeated until a satisfactory combination of position and rate feedback gains was determined.

a. X Axis Isolation

The NPADS X axis was isolated using two rails to prevent rotation and motion in the Y direction, Figure 42. In addition, the rotation and Y control gains were set to zero to conserve air by preventing unnecessary thruster firings.

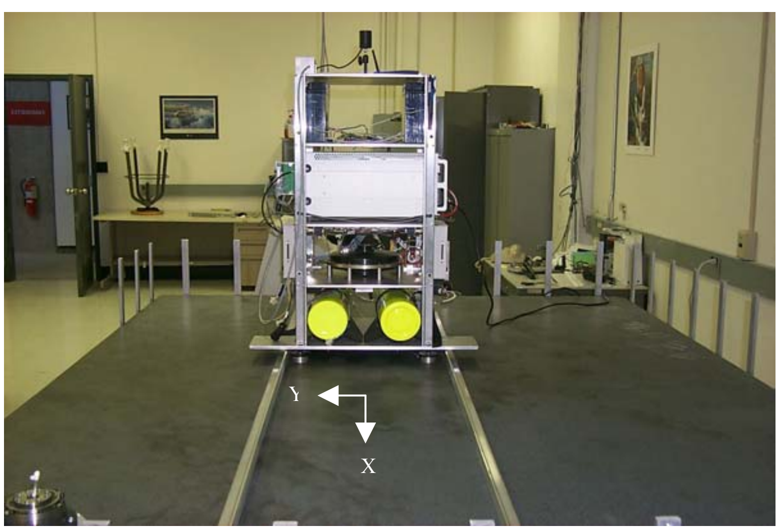

Figure 42 NPADS X Axis Isolation Test

Starting with the control gains used during Simulink modeling, the control gains were improved based on the observed performance. Due to a difference in the way the derivative gain is applied, $K_{d(Labview)} \approx (0.00185) K_{d(Simulink)}$. For a more detailed description of the LabView PID control functions, see Reference 9. The best vehicle response was obtained with K_p=4.0 and K_d=0.08. Figure 43 shows the rapid response to a commanded X position of 20 inches.

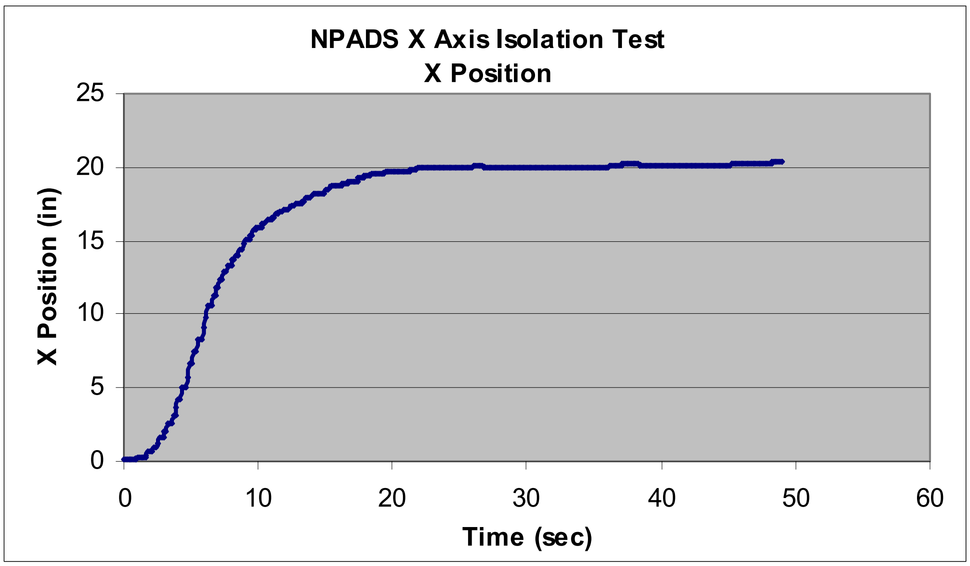

Figure 43 NPADS X Axis Isolation Position Response

As expected, the velocity plot, Figure 44, shows a rapid increase in vehicle velocity through approximately half the maneuver followed by a rapid decrease as the vehicle approaches the commanded position. The majority of the thruster activity, Figure 45, occurs during the initiation and termination of the maneuver, characteristic of a bang-bang thruster control scheme. Thrusters 1 and 8 are on continuously to get the vehicle moving and thrusters 4 and 5 stop the vehicle once it reaches the commanded position. The thruster 4 and 5 activity beyond approximately 20 seconds is most likely due to the difficulty in leveling the granite table.

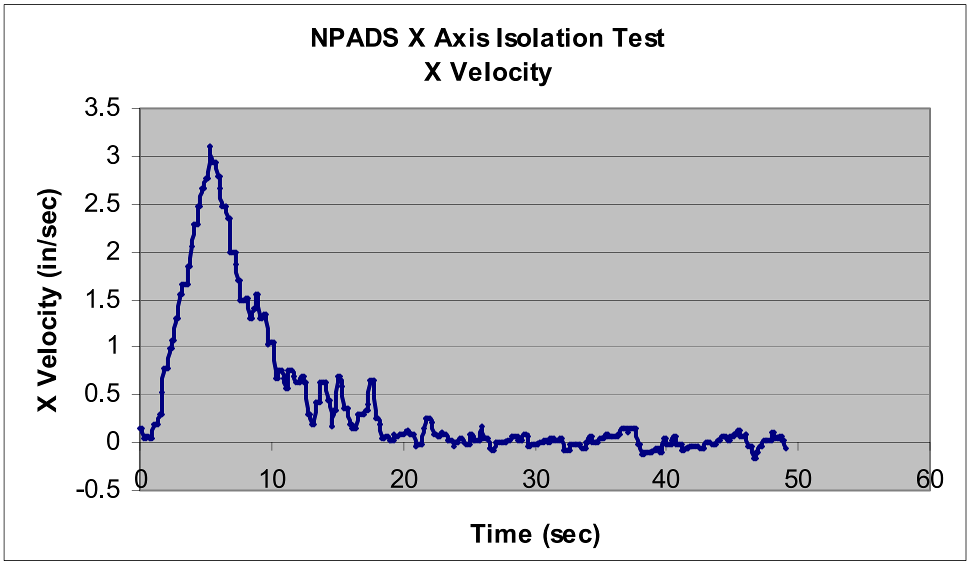

Figure 44 NPADS X Axis Isolation Velocity Response

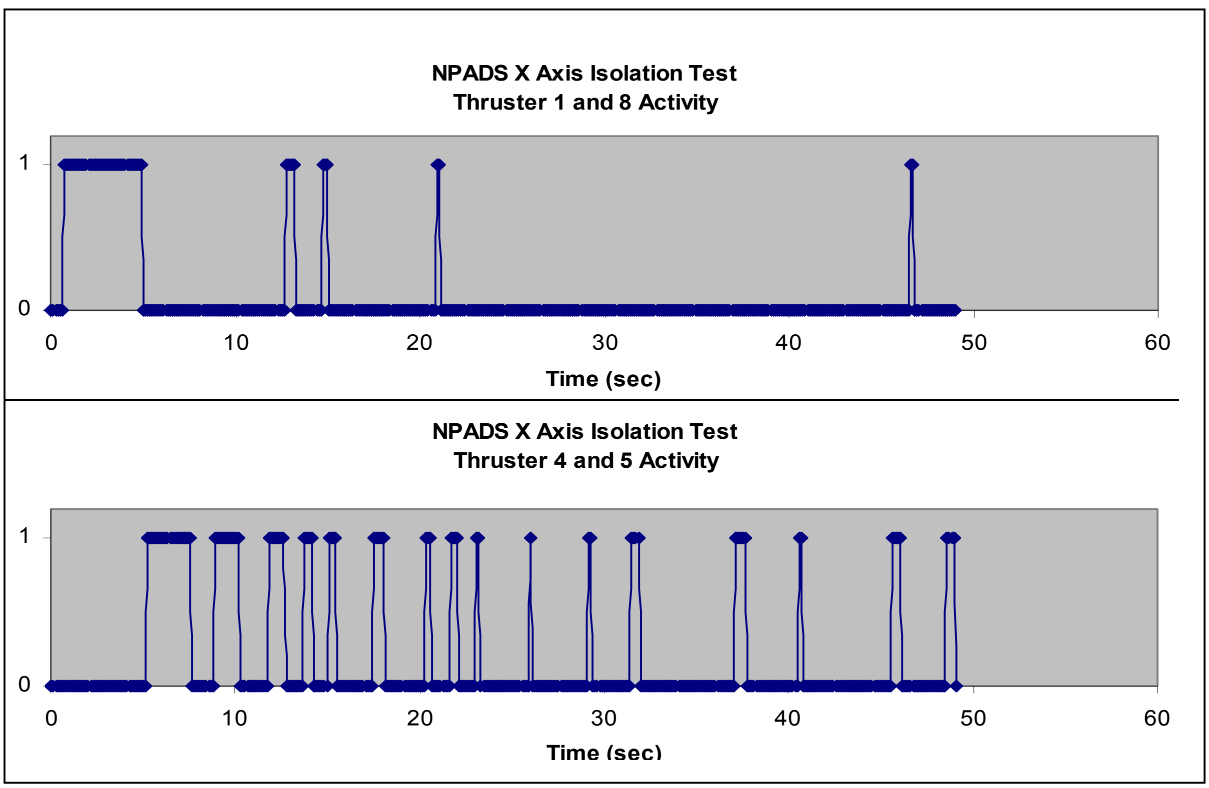

Figure 45 NPADS X Axis Isolation Thruster Activity

b. Y Axis Isolation

Although the LabView code and gains are identical to that of the X axis, the Y axis was tested to ensure no programming errors exist and compare the response. The Y axis was isolated using rails as depicted in Figure 46. Once again, the other degrees of freedom control gains were set to zero to conserve thruster air.

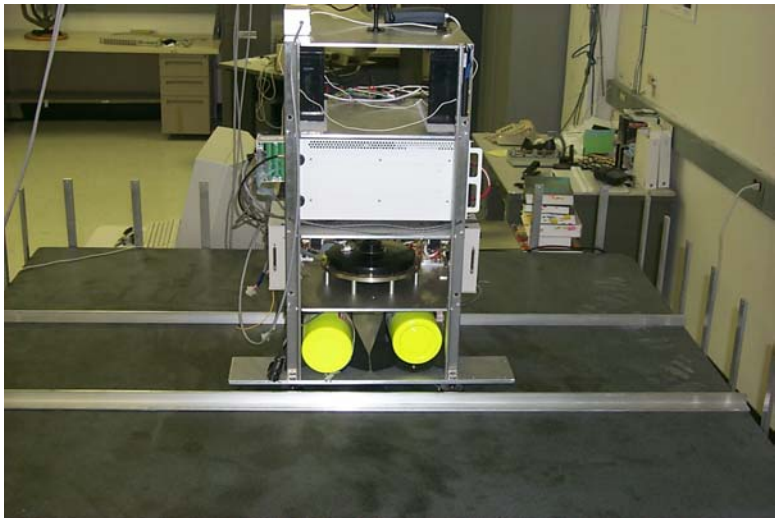

Figure 46 NPADS Y Axis Isolation Test

As expected, the vehicle response to a commanded Y position of -20 inches, Figure 47, was identical to the X axis response. The corresponding velocity response and thruster activity are included as Figure 48 and Figure 49 respectively.

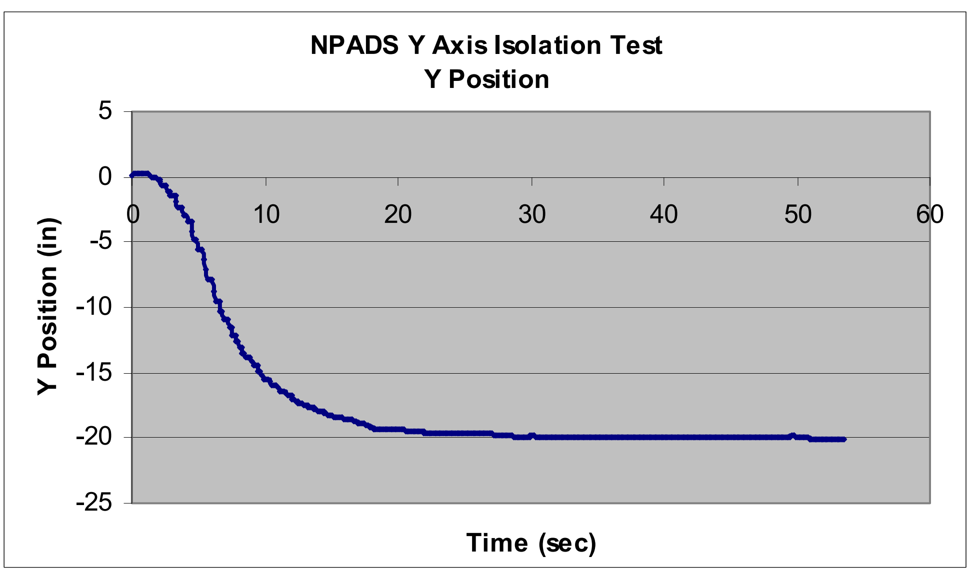

Figure 47 NPADS Y Axis Isolation Position Response

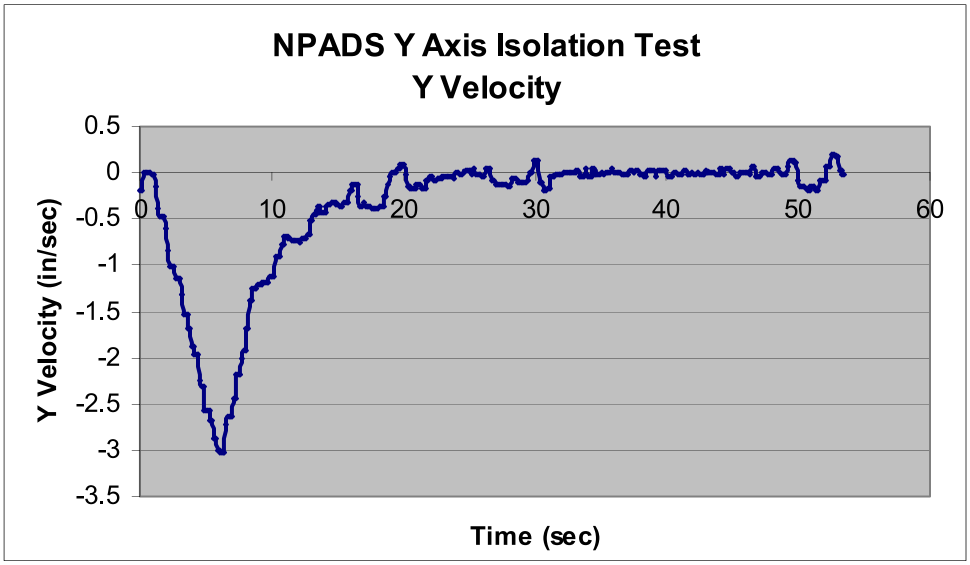

Figure 48 NPADS Y Axis Isolation Velocity Response

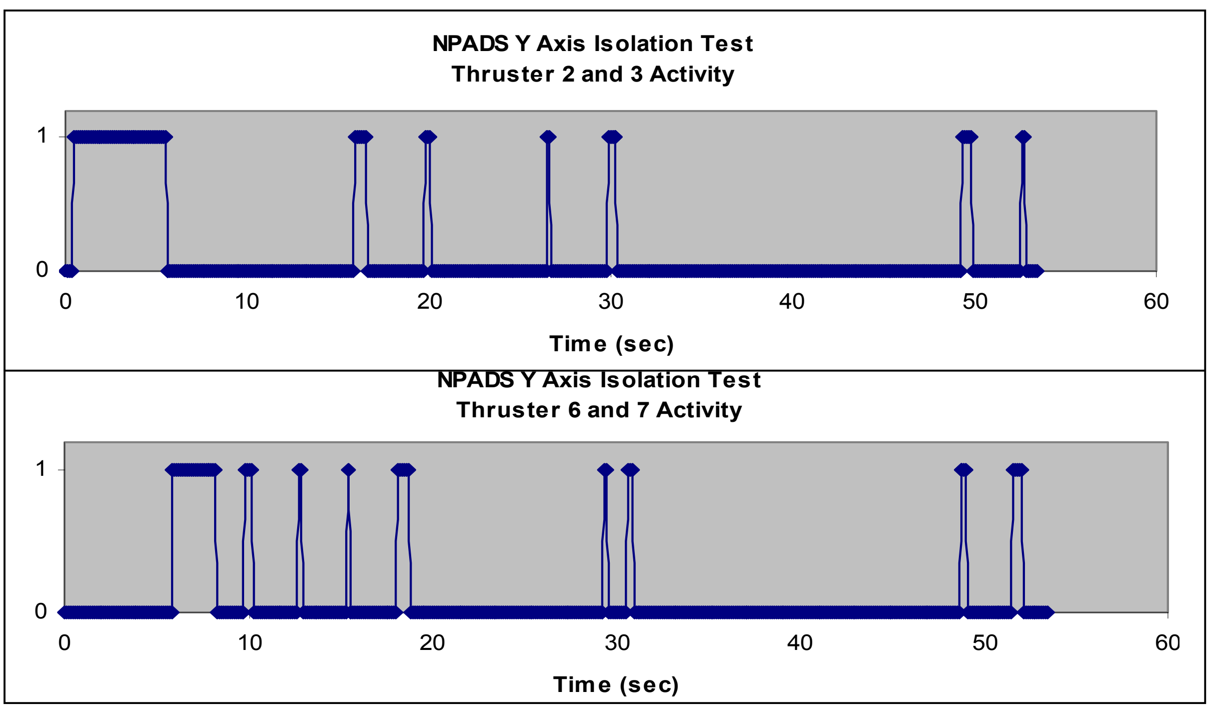

Figure 49 NPADS Y Axis Isolation Thruster Activity

c. Rotation Isolation

The NPADS rotational degree of freedom was isolated by setting the X and Y control gains to zero. Due to the possibility of data contamination, no attempt was made to prevent the vehicle from translating in the X and Y directions during the rotation tests. Once again, the Simulink simulation model gains were used as a starting point and improved based on the vehicle response to commands. The best response was obtained using K_p=1 and K_d=0.15. Figure 50 shows the resultant response to a commanded 45 degree rotation.

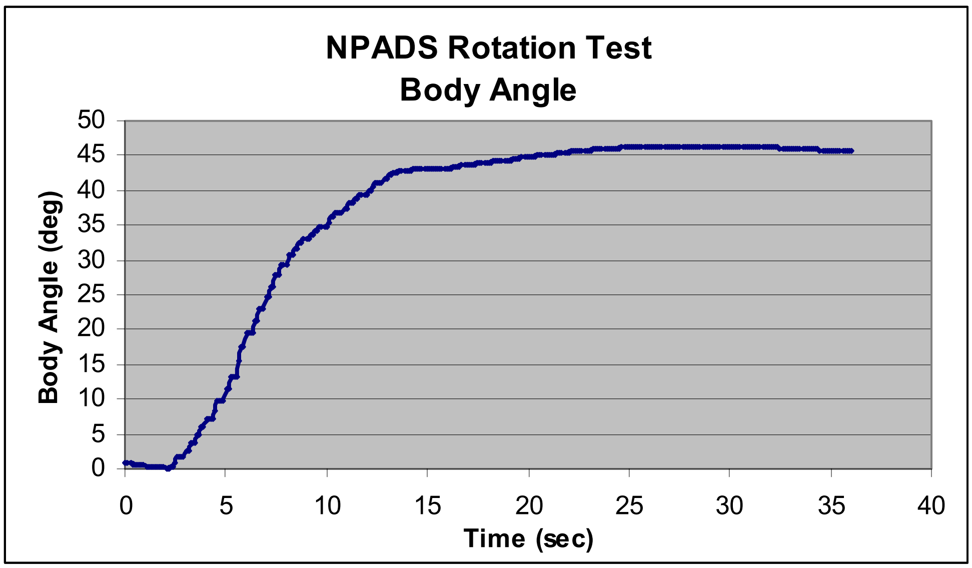

Figure 50 NPADS Rotation Isolation Response

The angular rate response, Figure 51, shows a rapid acceleration through the first half of the maneuver and a corresponding deceleration through the second half, as the vehicle approached the commanded rotation angle. The corresponding thruster activity is depicted in Figure 52. Thrusters 2, 4, 6 and 8 come on at the beginning of the maneuver and thrusters 1,3,5 and 7 stop the resultant rotation, again, characteristic of a bang-bang control scheme. The use of four thrusters for rotation results in an almost unacceptable use of air during large rotations. In the future, consideration should be given to using the reaction wheel for rotation. This would not only save thruster air but prevent thruster saturation and improve the vehicle response.

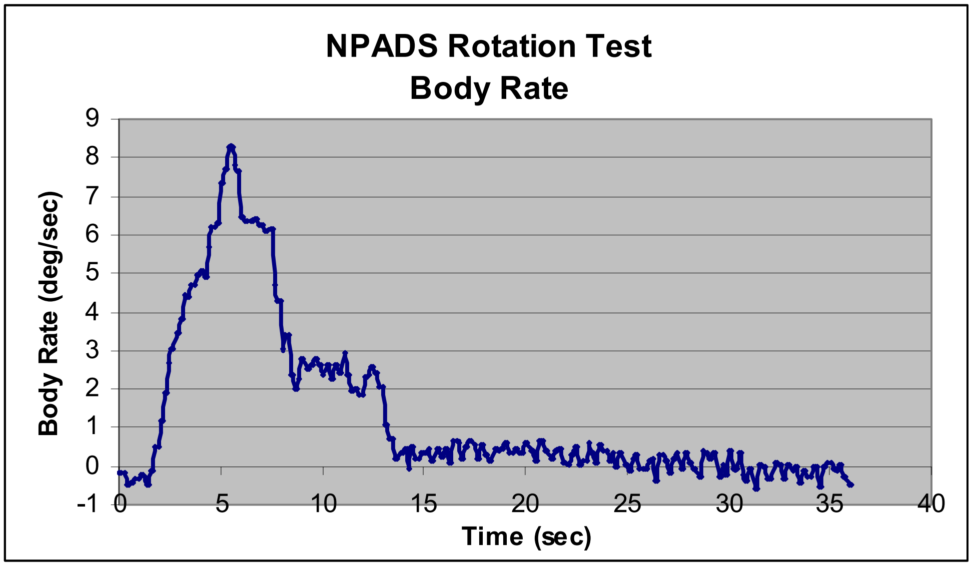

Figure 51 NPADS Rotation Isolation Angular Rate Response

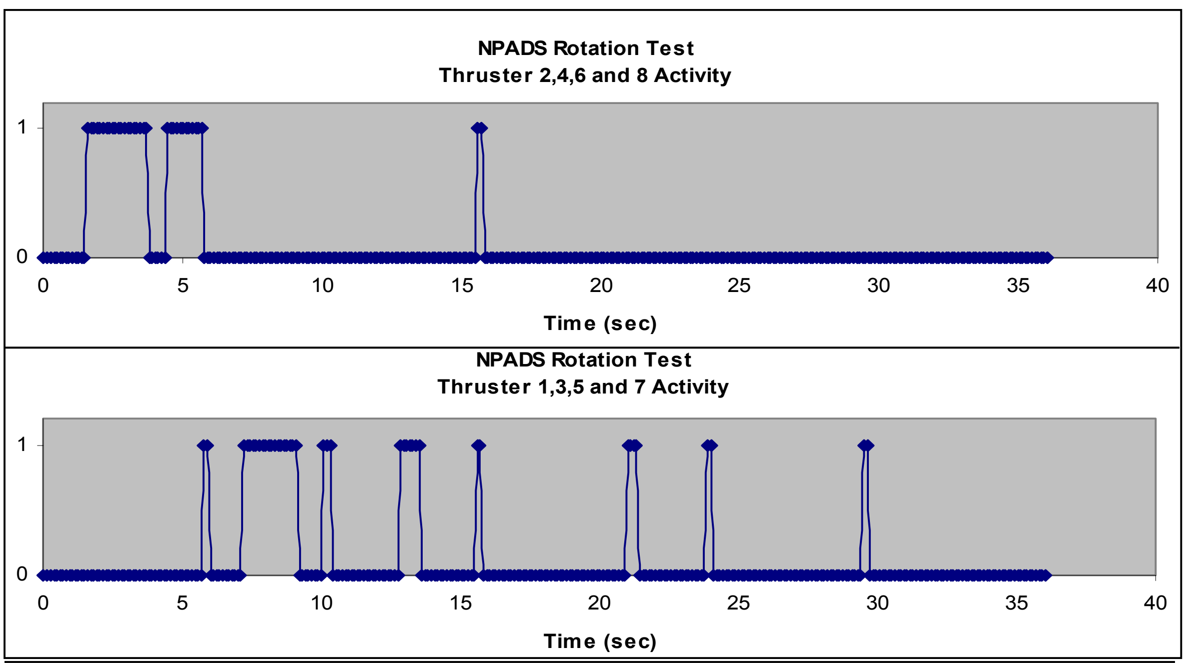

Figure 52 NPADS Rotation Isolation Thruster Activity

2. Fully Autonomous Operation

Once the final control gains were determined, the vehicle was tested under normal operating conditions. While satisfactory results were obtained throughout most of the testing, several response issues were noted and should be corrected. Table 10 lists the control gains used for the final test.

Table 10 NPADS Feedback Gains

DOF	K_d	K_p
X	4.0	0.08
Y	4.0	0.08
θ	1.0	0.15

Figure 53 shows the response to a combined X, Y and rotation (θ) command. The vehicle arrives at the commanded position fairly quickly, within one minute, and maintains that position within ±1 in and ±1 deg. As the relatively large 180 deg rotation begins, fairly large fluctuations in the X and Y positions were noted. Although other tests revealed much better results to smaller translations and rotations, this test is included to point out some of the required improvements to the vehicle control algorithm.

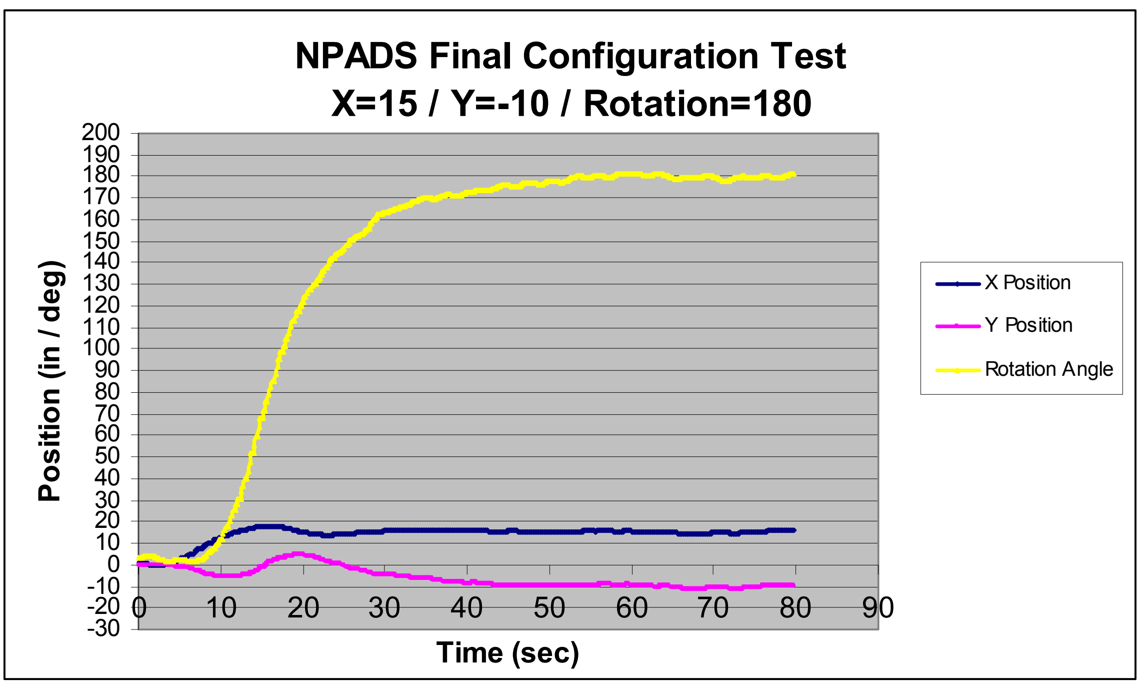

Figure 53 NPADS Final Configuration Response

The vehicle rate response, depicted in Figure 54, shows the angular rate oscillating as the vehicle approaches the desired position and tries to maintain that position. This is most likely due to the minimum impulse available from the thrusters. The oscillation could be smoothed out by either increasing the speed at which the control program runs or decreasing the thruster air pressure. While increasing the speed of the control computer would be the best choice, it would require running LabView Real-time which is not compatible with the NPADS vision system at this time, but will be available in the future. In order to reduce the thruster air pressure below 150 psi, a second pressure regulator could be added to the vehicle.

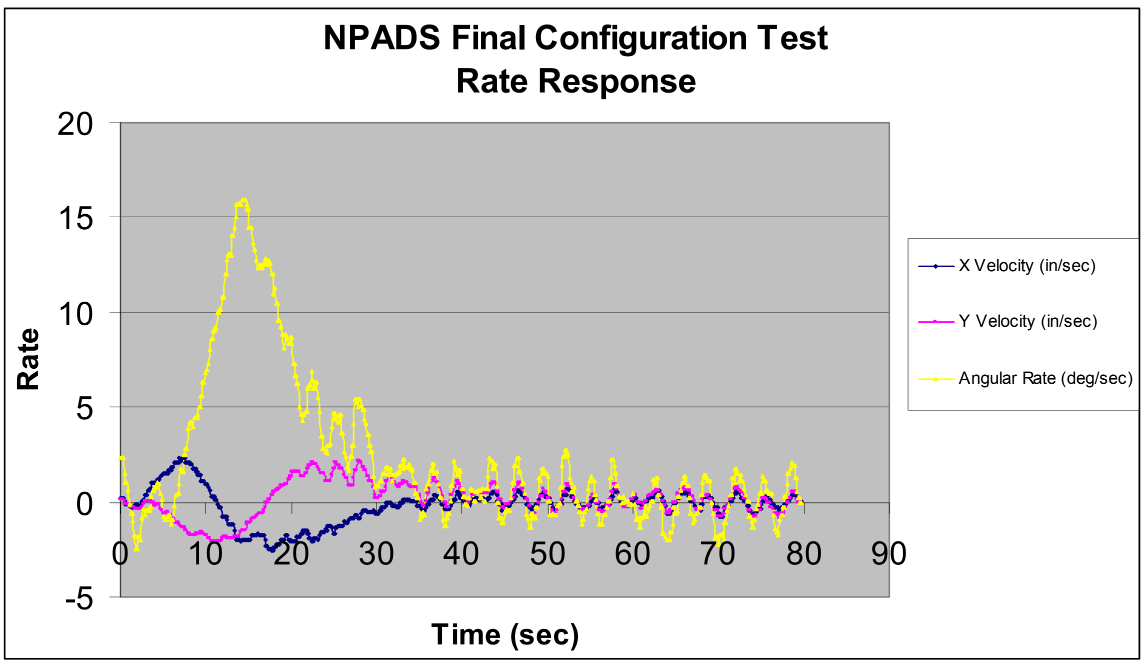

Figure 54 NPADS Final Configuration Rate Response

Figure 55 shows the thruster activity during the maneuver. As soon as the large rotation begins, approximately 8 seconds into the maneuver, all of the thrusters become saturated due to the long on time required for rotation. This causes fluctuations in the X and Y response until approximately 2/3 of the way through the rotation. In order to smooth out the X and Y response, two thrusters could be used for rotation based on the desired direction of the rotation and translation commands. In addition, the reaction wheel could be used exclusively for rotation, decreasing the thruster duty cycle.

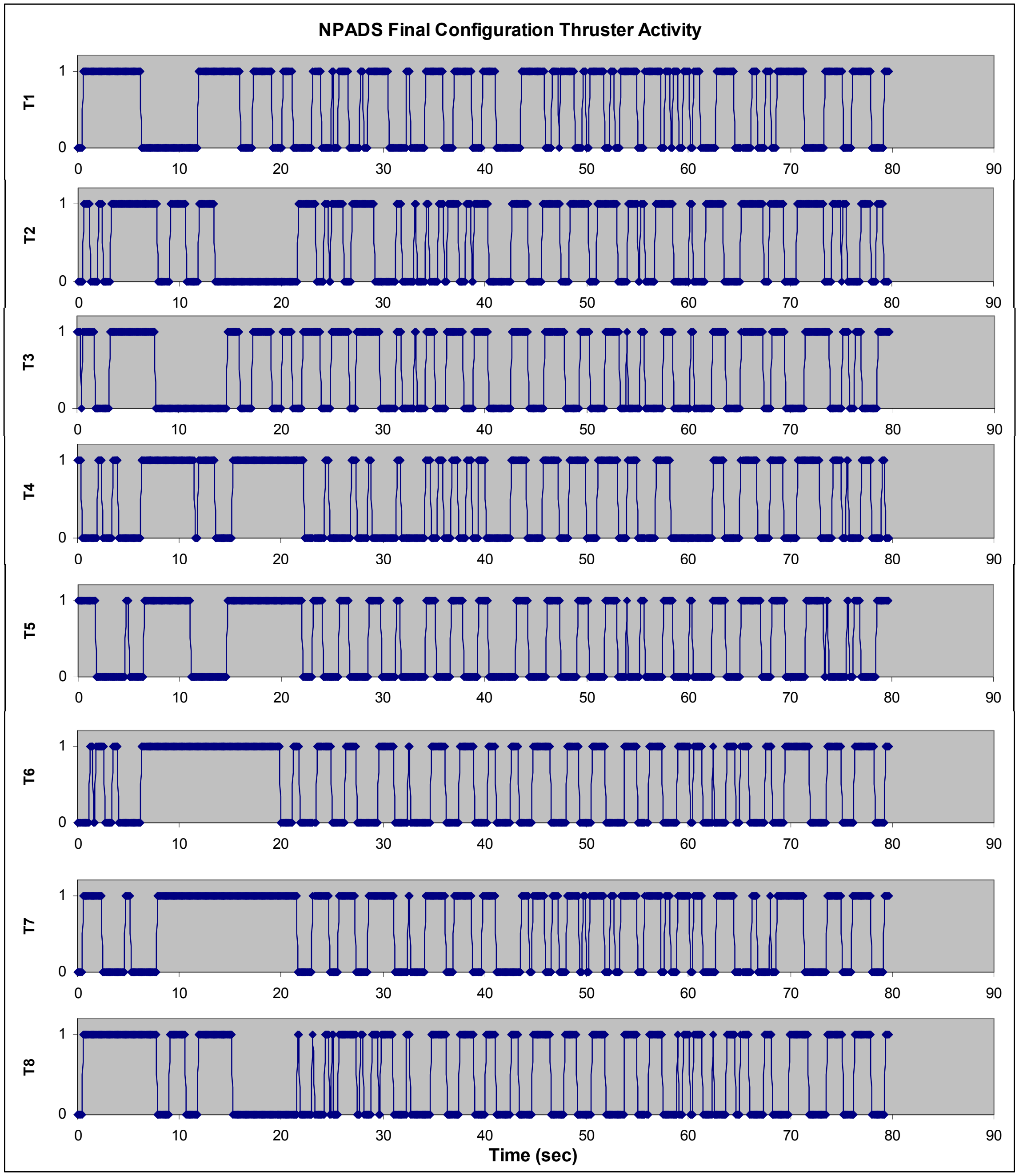

Figure 55 NPADS Final Configuration Thruster Activity

THIS PAGE INTENTIONALLY LEFT BLANK

VI. SUMMARY AND CONCLUSIONS

A. SUMMARY

The objective of this thesis was to design, construct and develop the initial autonomous control algorithm for the NPS Planar Autonomous Docking Simulator (NPADS) Servicing Vehicle. Following the construction and hardware integration, MATLAB Simulink was used to develop the initial PD control scheme, which included the required Pulse Width Modulation thruster control. NPADS was initial controlled using a manual control program which enabled a user to control thrusters, or combinations of thrusters, and the reaction wheel. Following successful modeling and manual control tests, the first autonomous control algorithm, a PD controller, was developed and tested.

B. NPADS IMPROVEMENTS

The following improvements to the NPADS Servicing Vehicle design are recommended:

- Explore the possibility of creating a larger air bearing surface on which to operate the simulator. The existing granite table will prove to be too small for advanced research in target rendezvous and capture.
- Add a pressure regulator to control the thruster air pressure. The thruster air supply proved to be the limiting factor in the amount of time the servicing vehicle could operate.
- Explore the possibility of creating a more efficient nozzle for the NPADS thrusters. Increasing the force generated by each individual thruster would help conserve thruster air.
- When it becomes available, use LabView Real-time to control the vehicle. This will increase the speed at which the control algorithm runs allowing for increased accuracy and shorter duration thruster firings. As of the

writing of this thesis, the IMAQ vision system did not work with LabView Real-time.

- Investigate the possibility of using two thrusters for vehicle rotation, vice four. Another alternative is to use the reaction wheel exclusively for rotation. The existing control program uses four thrusters for rotation causing thruster saturation and variations in the X and Y position during rotation.

C. FOLLOW-ON RESEARCH

The completion of the NPADS servicing vehicle opens the door for numerous research topics at NPS. The NPADS manipulators, or arms, need to be integrated with the servicing vehicle and a docking target created for the first docking application tests. The Air Force Research Lab has a docking collar available for these tests. In addition, work can begin on a neural network based control scheme which is one of the stated goals of the NPADS research. Machine Vision, Advanced Neural Network Control, Control Optimization, Docking Target Design and Docking Collar Design are just a few of the research opportunities created with the NPADS project. In addition, the vehicle could be used in teaching basic controls and the spacecraft controls series. As a student tool, and as hardware supporting DOD interests, NPADS will prove to be an extremely valuable asset.

APPENDIX A: NPADS WIRING DATA

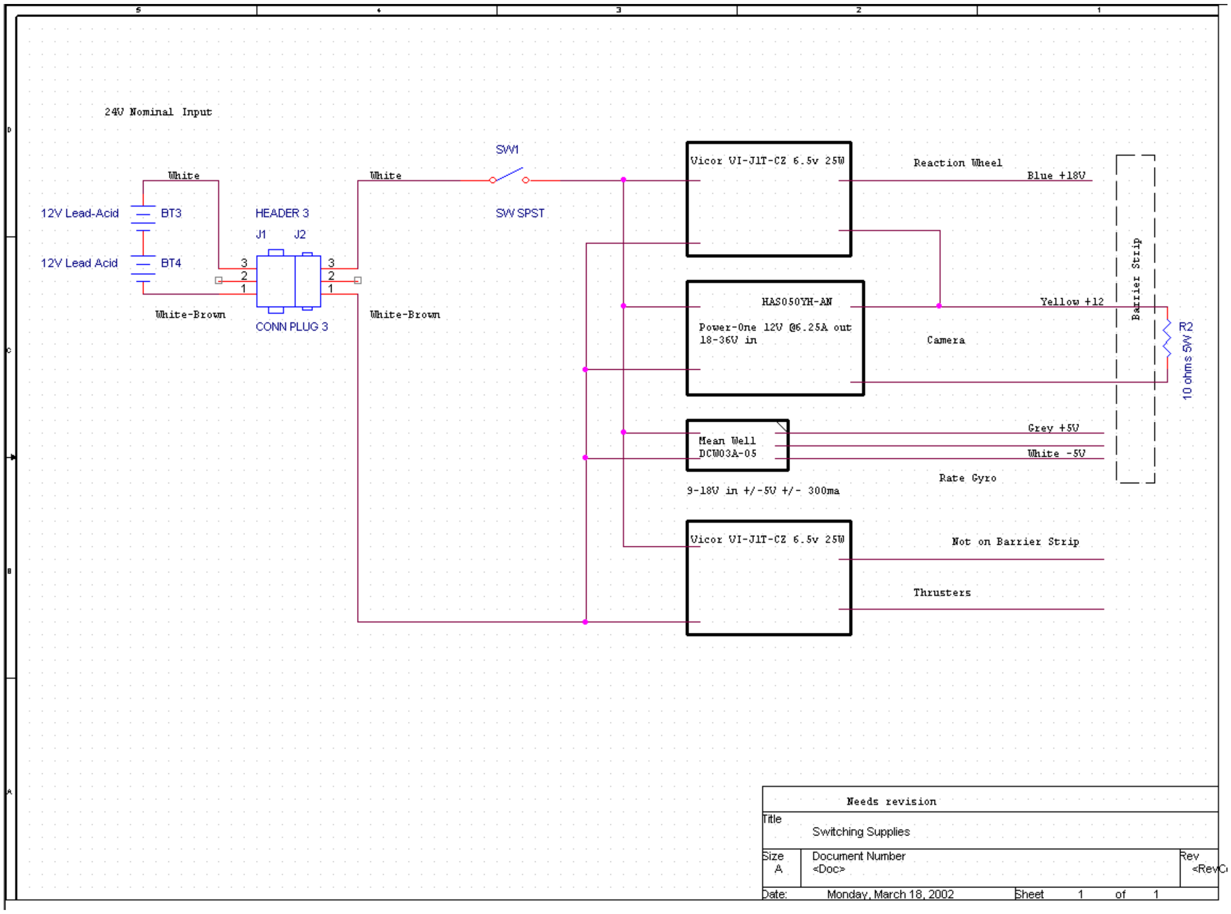

Figure 56   NPADS DC-DC Converter Wiring / Distribution Diagram

Table 11   PXI 6070E Multifunction I/O Card Pin Out

Pin Number	Signal Name	Pin Utilization	Notes
Reaction Wheel Control / Data Acquisition			
21 55	DAC1OUT AOGND	Torque Control Output Ground	Output voltage for control
25 59	ACH6 AIGND	Torque Feedback Input Ground	Input voltage for feedback
Rate Sensor Data Acquisition			
30 67	ACH3 AIGND	Rate Output Ground	Single ended input voltage

Table 12 PXI 6713 Analog Voltage Output Card Pin Out

Pin Number	Signal Name	Pin Utilization	Notes
Thruster Control			
52 53	DIO0 DGND	Thruster 1 Ground	* Digital I/O Lines (DIO) for thruster control.
17 53	DIO1 DGND	Thruster 2 Ground	
49 9	DIO2 DGND	Thruster 3 Ground	
47 9	DIO3 DGND	Thruster 4 Ground	
19 36	DIO4 DGND	Thruster 5 Ground	
51 36	DIO5 DGND	Thruster 6 Ground	
16 50	DIO6 DGND	Thruster 7 Ground	
48 50	DIO7 DGND	Thruster 8 Ground	
8 4	+5 V DGND	All Thrusters Ground	Master switch for thruster control. On when power is applied to computer.
Reaction Wheel RPM Measurement			
37	Counter 0	Hall Phase A	The 6713 counters convert Hall input to a frequency. (15 rpm/Hz)
42	Counter 1	Hall Phase B	
18	DGND	Ground	

Table 13 Rate Sensor Harness Design

Harness	Wire	Function	Connector Pin	Signal	Notes
Green (Power)	Green	+5 volts input	3	+5 volts	Connected to power barrier strip on third shelf
	Black	Ground	4		
	Red	-5 volts input	9	-5 volts	
	White	Ground	10		
Blue (Signal)	Green	Rate Output	7	±2.5 volts	Connected to 6070E Card
	White	Signal Ground	8		
	Black	BIT Output	5		Unused
	Red	Self Test	2		Unused

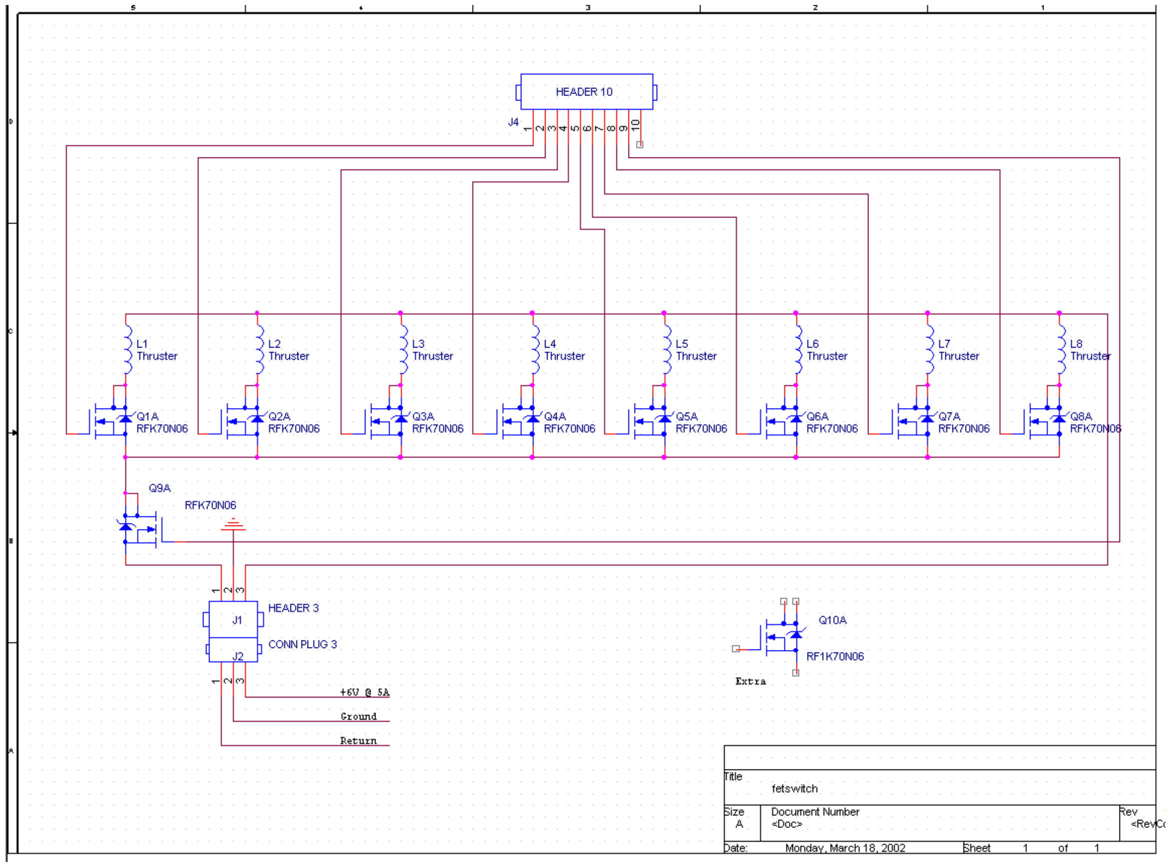

Figure 57 NPADS Thruster Wiring Diagram

Table 14 Reaction Wheel Harness Design

Harness	Wire	Function	Connector Pin	Signal	Notes
Red (Power)	Green	+18 volts input	1	+18 volts	Connected to power barrier strip on third shelf
	Black	Ground	7		
	Red	+18 volts input	6	+18 volts	
	White	Ground	2		
Blue (Signal)	Red	Torque Command	14	±2.0 volts	Connected to 6070E Card
	Black	Ground	15		
	Green	Torque Feedback	11	±5.0 volts	
	White	Ground	12		
Green (Hall)	Red	Hall Phase A	8	0-5 volts	Only Phase A connected to 6070E card for RW RPM.
	Green	Hall Phase B	9	0-5 volts	
	White	Hall Phase C	10	0-5 volts	
	Black	Hall Ground	5		
White (Disable)	Red	Wheel Disable	4		Not used at this time
	Black	Chassis Ground	3		

THIS PAGE INTENTIONALLY LEFT BLANK

Table 15 NPADS Mass Properties

	Weight (lb)	Mass (slugs)	Size X	Size Y	Size Z	Diameter	CM X	CM Y	CM Z	MOI Gx	MOI Gy	MOI Gz
Main Feet and Hose	0.755	0.0234472			0.75	2.125	7.25	7.25	-0.5	0.007717	0.007717	0.013235
Main Feet and Hose	0.755	0.0234472			0.75	2.125	7.25	-7.25	-0.5	0.007717	0.007717	0.013235
Main Feet and Hose	0.755	0.0234472			0.75	2.125	-7.25	7.25	-0.5	0.007717	0.007717	0.013235
Main Feet and Hose	0.755	0.0234472			0.75	2.125	-7.25	-7.25	-0.5	0.007717	0.007717	0.013235
Base Plate	9.0327	0.28051863	15	15	0.375		0	0	-1.5	5.259724	5.259724	10.51945
Arm Pad section of Base Plate	1.0036	0.0311677	5	5	0.375		5	10	-1.5	0.064933	0.064933	0.129865
Arm Pad section of Base Plate	1.0036	0.0311677	5	5	0.375		5	-10	-1.5	0.064933	0.064933	0.129865
Air Tank Mounting Plates	0.43	0.01335404	12	6	0.0625		0	4	-2	0.040062	0.160248	0.200311
Air Tank Mounting Plates	0.43	0.01335404	12	6	0.0625		0	-4	-2	0.040062	0.160248	0.200311
Long 19 cu ft Air Tank (Full)	11.17	0.34689441	19			4.25	-1.5	4	-4.5	1.566445	11.21896	11.21896
Short 19 cu ft Air Tank (Full)	10.37	0.32204969	19			4.25	-1	-4	-4.5	1.454256	10.41546	10.41546
Air Tank Regulator	1.84	0.05714286	1.75	2.5	5		-13.5	4	-5.25	0.14881	0.133631	0.044345
Air Tank Regulator	1.84	0.05714286	1.75	2.5	5		-13.5	-4	-5.25	0.14881	0.133631	0.044345
Rate Sensor and Mount	0.222	0.00689441	0.5			1.5	0	0	-7.5	0.003878	0.002083	0.002083
Vertical Support	1.53	0.04751553	1.25	1.25	29		7.25	7.25	-16.25	3.336234	3.336234	0.012374
Vertical Support	1.53	0.04751553	1.25	1.25	29		7.25	-7.25	-16.25	3.336234	3.336234	0.012374
Vertical Support	1.53	0.04751553	1.25	1.25	29		-7.25	7.25	-16.25	3.336234	3.336234	0.012374
Vertical Support	1.53	0.04751553	1.25	1.25	29		-7.25	-7.25	-16.25	3.336234	3.336234	0.012374
Pressure Regulator	1.49	0.04627329			5	2.5	-8.75	-8.75	-7	0.114478	0.114478	0.036151
Reaction Wheel Plate	5.55	0.17236025	15	15	0.25		0	0	-8.375	3.231755	3.231755	6.463509
Reaction Wheel with Standoffs	7.28	0.22608696			3	10.25	0	0	-10	1.654144	1.654144	2.969158
Power Strip	0.33	0.01024845	1	6	0.25		-6.5	0	-8.5	0.030799	0.000907	0.031599
Reaction Wheel Shunt	0.25	0.00776398	1.5	1.75	3		-3.5	-5.5	-10.5	0.007804	0.007279	0.003437
Arm UMI	1.94	0.06024845	7	1.5	6		0	8.5	-12	0.192042	0.42676	0.257311
Arm UMI	1.94	0.06024845	7	1.5	6		0	-8.5	-12	0.192042	0.42676	0.257311
Thruster Plate w/ circuitry	8.92	0.27701863	15	15	1.5		0	0	-14.75	5.24604	5.24604	10.3882
PXI	20	0.62111801	10.75	15	7.5		0	0	-19	14.55745	8.892987	17.62746
Battery Plate	5.57	0.17298137	15	15	0.25		0	0	-23.375	3.244302	3.244302	6.486801
Battery	14.83	0.46055901	7	3	6.5		0	5.75	-27	1.966971	3.502167	2.226035
Battery	14.83	0.46055901	7	3	6.5		0	-5.75	-27	1.966971	3.502167	2.226035
Power Strip	0.33	0.01024845	1	6	0.25		-6.5	0	-23.75	0.030799	0.000907	0.031599
Top Plate	5.55	0.17236025	15	15	0.25		0	0	-30.625	3.232652	3.232652	6.463509
Proxim Ethernet	0.62	0.01925466	3.25	5.5	1		-5	-4	-31.5	0.050142	0.018553	0.065486
Camera (Star Sensor)	0.46	0.01428571			5	1.5	0	0	-35	0.031771	0.031771	0.004018
Camera (Docking)	1.2	0.03726708	6.5	2.5	2		5	0	-34	0.031832	0.143634	0.150621
Total Weight	**137.5719**	**4.27241925**					-0.6402	-0.0995	-15.082	57.94971	74.66691	88.69567

	dx	dy	dz	m*(dy^2+dz^2)	m*(-dxdy)	m*(-dxdz)	m*(dx^2+dz^2)	m*(-dydz)	m*(dx^2+dy^2)
Main Feet and Hose	-7.89019	-7.34953	-14.5822	6.252312401	-1.359683518	-2.69773988	6.445504128	-2.51288	2.726220849
Main Feet and Hose	-7.89019	7.15047	-14.5822	6.184635246	1.322856946	-2.69773988	6.445504128	2.444823	2.658543694
Main Feet and Hose	6.609815	-7.34953	-14.5822	6.252312401	1.139042482	2.25996733	6.010198046	-2.51288	2.290914766
Main Feet and Hose	6.609815	7.15047	-14.5822	6.184635246	-1.108191899	2.25996733	6.010198046	2.444823	2.223237611
Base Plate	-0.64019	-0.09953	-13.5822	51.75145648	-0.017873944	-2.439136714	51.86364457	-0.37921	0.117745822
Arm Pad section of Base Plate	-5.64019	-10.0995	-13.5822	8.928783325	-1.77541262	-2.387629409	6.741159356	-4.27538	4.170618481
Arm Pad section of Base Plate	-5.64019	9.90047	-13.5822	8.804698753	1.740419621	-2.387629409	6.741159356	4.191113	4.046533909
Air Tank Mounting Plates	-0.64019	-4.09953	-13.0822	2.509877899	-0.035047116	-0.11184012	2.290921002	-0.71619	0.229902859
Air Tank Mounting Plates	-0.64019	3.90047	-13.0822	2.488611911	0.033345345	-0.11184012	2.290921002	0.681411	0.20863687
Long 19 cu ft Air Tank (Full)	0.859815	-4.09953	-10.5822	44.6759092	1.222745975	3.156286581	39.10240426	-15.0489	6.086410123
Short 19 cu ft Air Tank (Full)	0.359815	3.90047	-10.5822	40.96334566	-0.451979591	1.226241725	36.10548331	13.29273	4.941251749
Air Tank Regulator	12.85981	-4.09953	-9.83216	6.484426897	3.012525342	7.225127289	14.9740664	-2.30327	10.41034171
Air Tank Regulator	12.85981	3.90047	-9.83216	6.393428247	-2.866247119	7.225127289	14.9740664	2.191431	10.31934306
Rate Sensor and Mount	-0.64019	-0.09953	-7.58216	0.396421833	-0.000439295	-0.033465366	0.399179121	-0.0052	0.002893883
Vertical Support	-7.89019	-7.34953	1.167842	2.631383489	-2.755385142	0.437831431	3.022884605	0.40783	5.524659468
Vertical Support	-7.89019	7.15047	1.167842	2.494236407	2.68075646	0.437831431	3.022884605	-0.39678	5.387512386
Vertical Support	6.609815	-7.34953	1.167842	2.631383489	2.308258275	-0.366782853	2.140741153	0.40783	4.642516016
Vertical Support	6.609815	7.15047	1.167842	2.494236407	-2.245739875	-0.366782853	2.140741153	-0.39678	4.505368934
Pressure Regulator	8.109815	8.65047	-8.08216	6.485290213	-3.246243154	3.032973773	6.06598294	3.235172	6.506012377
Reaction Wheel Plate	-0.64019	-0.09953	-6.70716	7.755499587	-0.010982363	-0.74008447	7.824431788	-0.11506	0.072347063
Reaction Wheel with Standoffs	-0.64019	-0.09953	-5.08216	5.841687627	-0.014405694	-0.735578976	5.932106803	-0.11436	0.09489849
Power Strip	5.859815	-0.09953	-6.58216	0.444113457	0.005977161	0.395284917	0.795917263	-0.00671	0.352006851
Reaction Wheel Shunt	2.859815	5.40047	-4.58216	0.389450687	-0.119909507	0.101740081	0.226511726	0.192126	0.289934931
Arm UMI	-0.64019	-8.59953	-3.08216	5.027829848	-0.331685297	-0.118879339	0.597034014	-1.59689	4.480179937
Arm UMI	-0.64019	8.40047	-3.08216	4.823948362	0.324007537	-0.118879339	0.597034014	1.559927	4.276298451
Thruster Plate w/ circuitry	-0.64019	-0.09953	-0.33216	0.033307324	-0.017650933	-0.058905935	0.144095654	-0.00916	0.116276721
PXI	-0.64019	-0.09953	3.917842	9.539996239	-0.039576082	1.557853898	9.788400566	0.2422	0.260710136
Battery Plate	-0.64019	-0.09953	8.292842	11.89785532	-0.011021939	0.918350326	11.96703593	0.142776	0.072607773
Battery	-0.64019	-5.84953	11.91784	81.1744285	-1.724693366	3.513893294	65.60423583	32.10731	15.94770104
Battery	-0.64019	5.65047	11.91784	80.12012383	1.666002037	3.513893294	65.60423583	-31.0147	14.89339637
Power Strip	5.859815	-0.09953	8.667842	0.770082621	0.005977161	-0.520538616	1.121886427	0.008841	0.352006851
Top Plate	-0.64019	-0.09953	15.54284	41.64048672	-0.010982363	1.715035871	41.70941892	0.266637	0.072347063
Proxim Ethernet	4.359815	3.90047	16.41784	5.482941341	-0.327431775	-1.378224396	5.555999614	-1.23302	0.658926233
Camera (Star Sensor)	-0.64019	-0.09953	19.91784	5.667576363	-0.00091025	0.182158695	5.673289663	0.02832	0.005996333
Camera (Docking)	-5.64019	-0.09953	18.91784	13.33768923	-0.020920485	3.97640253	14.52284886	0.07017	1.185897978
Total Weight				488.9544026	-3.030498982	25.86428941	454.4521265	1.278052	120.1301968

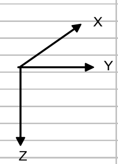

MOI G

x	y	z
57.95	0	0
0	74.6669	0
0	0	88.696

Parallel

x	y	z
488.9544	-3.0305	25.86429
-3.0305	454.4521	1.278052
25.86429	1.278052	120.1302

Ref p. 336 Baruh

Total MOI

x	**y**	**z**	
546.9041	**-3.030498982**	**25.86428941**	
-3.0305	**529.1190394**	**1.278051552**	in-lb-s^2
25.86429	**1.278051552**	**208.8258633**	
45.57534	**-0.252541582**	**2.155357451**	
-0.25254	**44.09325328**	**0.106504296**	ft-lb-s^2
2.155357	**0.106504296**	**17.40215527**	

THIS PAGE INTENTIONALLY LEFT BLANK

APPENDIX C: MANUAL CONTROL CODE

The LabView Manual Control Code is divided into three separate While loops. The thruster control loop, depicted in Figure 58, is controlled through actuation of a thruster control toggle switch on the Manual Control Panel. Once the toggle switch is turned on, each of the thruster control buttons sends a Boolean true or false, or on and off respectively, to the appropriate thruster digital write subroutine. The digital write subroutine converts the Boolean value into a digital 1 or 0, representing a on or off condition, and sends the value to the digital output pins of the PXI 6713 card for thruster control. In addition to individual thruster control, thrusters can be actuated two at a time and four at a time for translation and rotation respectively. Each of the green Boolean inputs depicted in Figure 58 corresponds to a thruster push button control on the Manual Control Panel, depicted in Chapter IV.

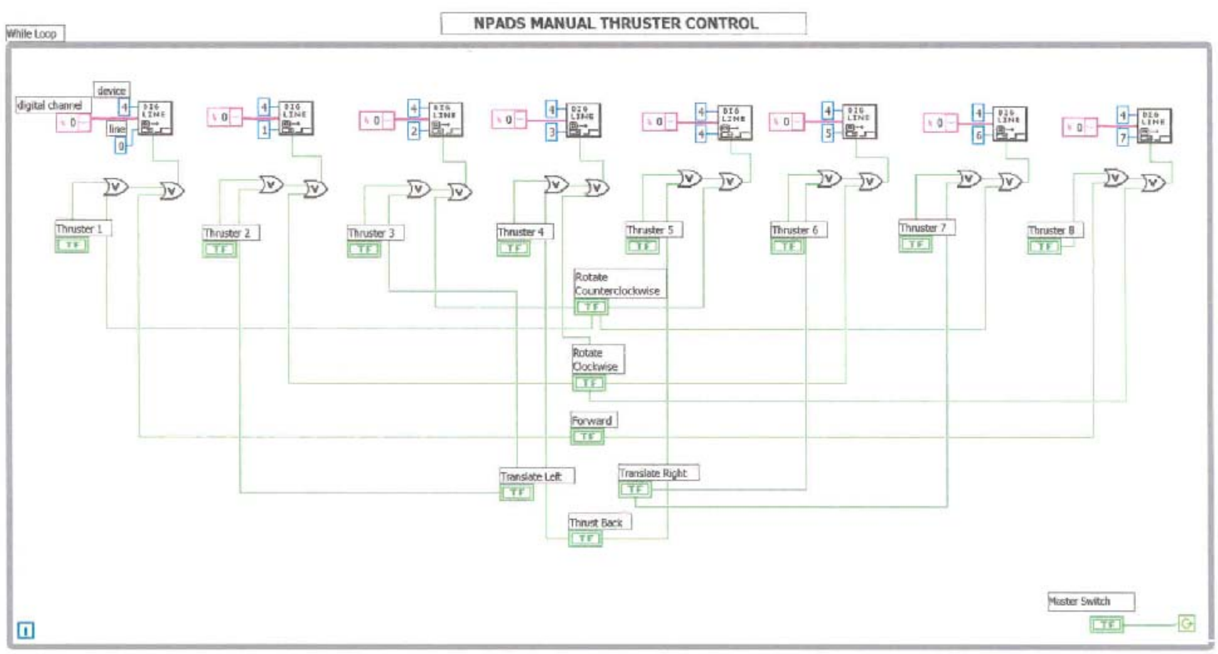

Figure 58 NPADS Manual Thruster Control Code

The reaction wheel control loop, depicted in Figure 59, is controlled through actuation of a reaction wheel control toggle on the Manual Control Panel. Once the toggle switch is turned on, a desired torque value can be commanded for positive or negative rotation. Once a value is entered, the reaction wheel will not be energized until the Torque Command push button is activated and held on the Control Panel. The value entered is then checked to ensure it is less than or equal to the maximum allowable torque of ±8 oz-in. In addition, the reaction wheel RPM is monitored by measuring the frequency from one of three hall sensors in the reaction wheel. In the event the frequency exceeds 133 Hz, or 1995 RPM, the reaction wheel will be de-energized and an over speed light will illuminate on the control panel. The limited 1995 RPM is well below the maximum 2350 required by the manufacturer and can be increased as required. Once all of the limits are verified, the commanded torque value is sent to an analog output subroutine, located on the far right of Figure 59, which sends the analog signal to the PXI 6070E multifunction I/O card to command the reaction wheel.

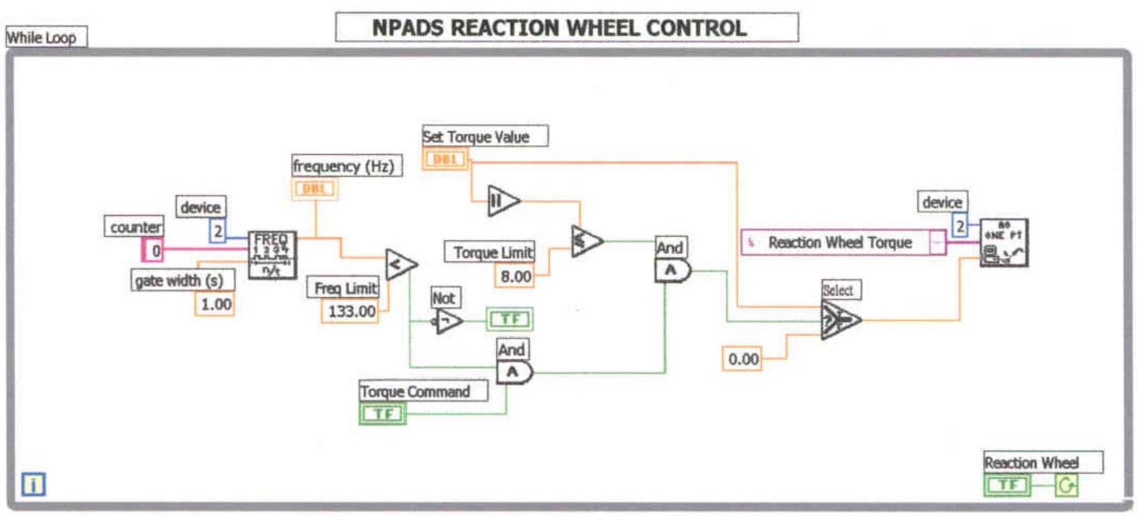

Figure 59 NPADS Manual Reaction Wheel Control Code

The third and final Manual Control While loop controls the output of the MEMS Rate Sensor on the NPADS vehicle, Figure 60. A toggle switch on the Control Panel activates the Rate Sensor While loop, causing the current angular velocity to be displayed in deg/sec. An analog read subroutine reads the angular acceleration input from the PXI 6070E card and displays the value to the screen.

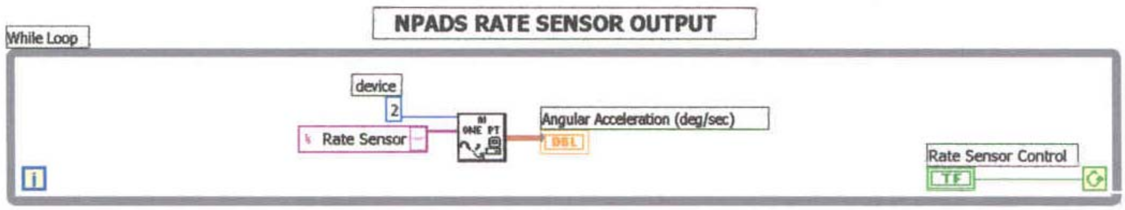

Figure 60 NPADS Manual Control Rate Sensor Output

All of the digital and analog input and output subroutines are built-in LabView functions. Prior to creating any control code, the PXI 6070E and 6713 cards were configured using the National Instruments Measurement and Automation Explorer. Having configured each of the cards, the input or output pins could easily be specified using the built-in functions. This greatly simplified the requirement to read or write from or to a required card.

THIS PAGE INTENTIONALLY LEFT BLANK

APPENDIX D: AUTONOMOUS CONTROL CODE

The NPADS Autonomous Control Algorithm is divided into several parts or subroutines as depicted in the following figures. The three major segments are Control Initialization, Figure 61, Rate Sensor Bias and Measurement, Figure 62, and PD Control Structure, Figure 63. The remaining segments are subroutines to the PD Control Structure.

A. CONTROL INITIALIZATION SEGMENT

The Control Initialization segment, Figure 61, runs each time the Autonomous Control algorithm is run. The purpose of this segment is to initialize the Rotation Memory Buffer, used to pass the current vehicle rotation angle from the Rate Sensor Bias and Measurement segment to the PD Control Structure, and initialize the eight thrusters to the off condition. Each thruster is commanded to the off condition to prevent the loss of thruster air in the event the thruster was on when the program was terminated.

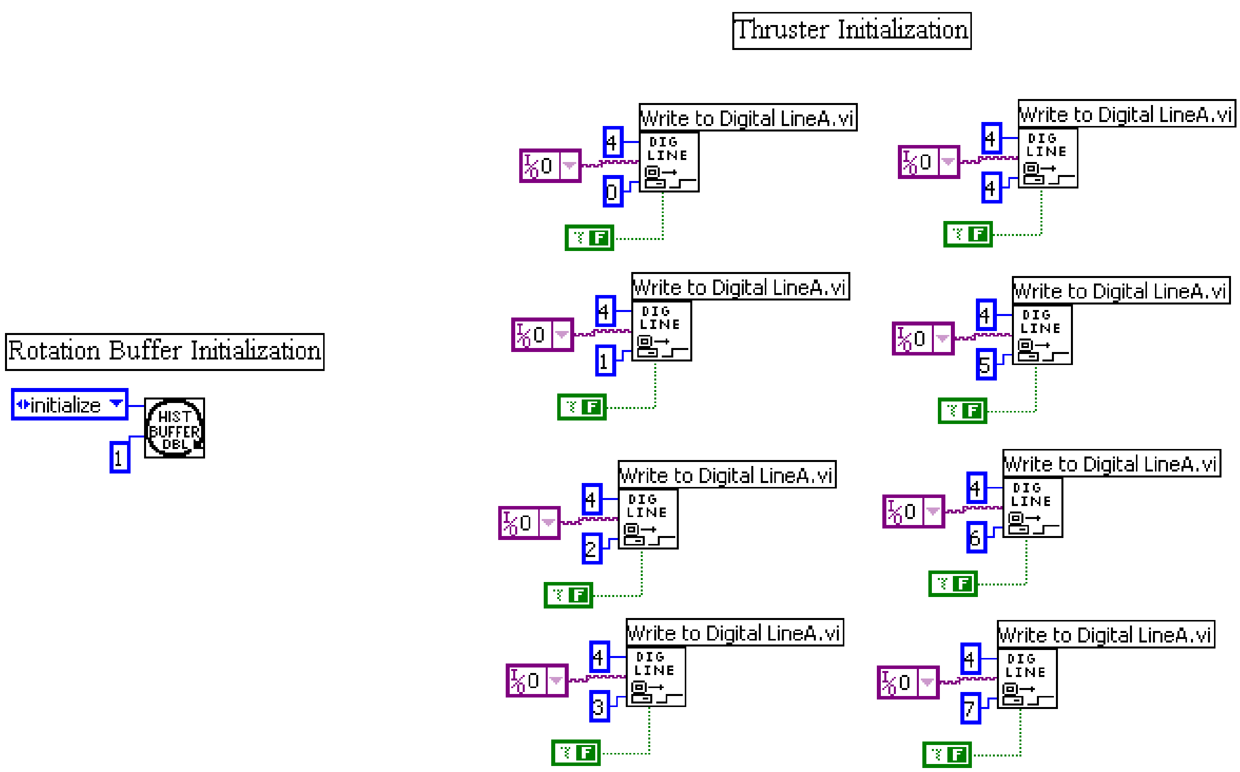

Figure 61 NPADS Autonomous Control Initialization Segment

B. RATE SENSOR BIAS AND MEASUREMENT SEGMENT

The Rate Sensor Bias and Measurement segment, Figure 62, finds the rate sensor bias upon program initiation and continuously sends the current rotation angle to the PD Control segment. With the exception of the rate sensor acquisition parameters, which set the desired sample rate from the rate sensor, the entire segment is located within a While loop so that it will continue to run throughout the program execution. Within the outer While loop are two Case statements, one for determining the rate bias and the other for sending the current rotation angle to the PD control segment. Upon program execution, the Boolean input to the case statements, labeled Begin Rate Control, is False causing the Rate Bias Case to run. Once a satisfactory rate bias has been determined, the user depresses the Begin Rate Control causing the current angular displacement to be sent to the PD control segment.

The Rate Bias Case reads 10,000 samples from the MEMS Rate Sensor and calculates the mean static angular acceleration. The mean static rate is then stored in a global variable, Rate Bias, and is subtracted from each rate sample in the Calculate Rotation Angle Case. The Bias Case uses a lowpass filter to remove rate sensor noise.

Upon initiation of Rate Sensor Control, the Bias Case is terminated and the Calculate Rotation Angle Case is initiated. The Calculate Rotation Angle Case continuously reads data from the MEMS Rate Sensor, via the PXI 6713 card, and subtracts the rate bias. The sampled data is then integrated, resulting in the angular displacement of the vehicle over the sample time. The angular displacement is then added to the previous angular displacement, via a shift register structure, resulting in a continuous total angular displacement. The instantaneous angular displacement is then stored in a Memory Buffer for use in the PD Control segment.

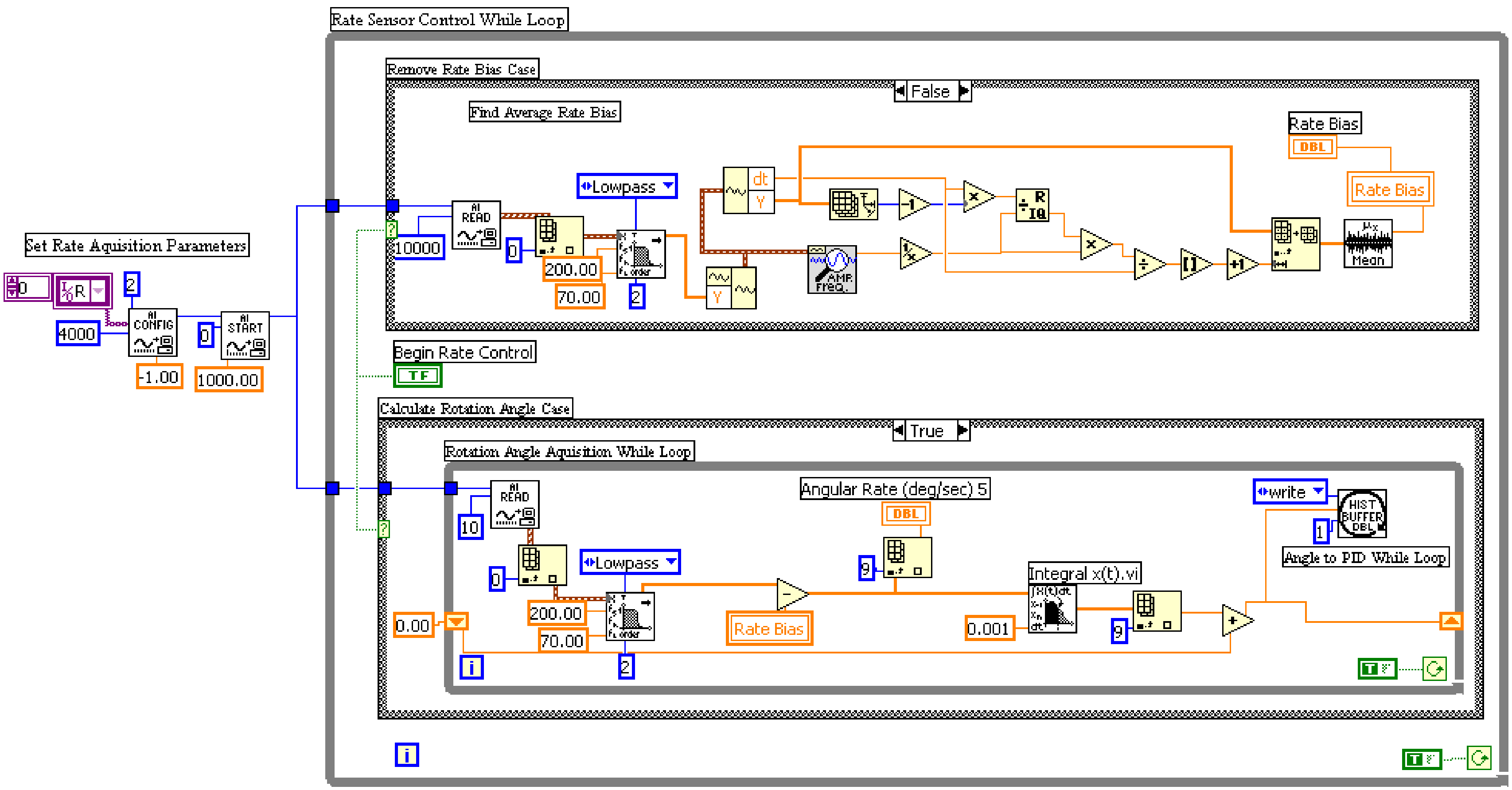

Figure 62 NPADS Autonomous Control Rate Sensor Bias and Measurement Segment

C. PD CONTROL STRUCTURE SEGMENT

The PD Control Structure segment is the heart of the NPADS Autonomous Control Algorithm and consists of the main program segment, Figure 63, and several subroutines within the segment.

1. Main Program

The Main Program is divided into three separate PD loop structures, as depicted in Figure 63. Each PD loop structure uses a built-in LabView subroutine called PID which takes the desired position, the set point, and the instantaneous position, the process variable, and calculates a controller action using the specified controller gains. The rates required for the derivative action are derived within the PID subroutine, eliminating the need for accelerometers at this time. While the PID subroutine can also calculate integral action, the integral action gain was set to zero, making it a true PD type controller. For a more detailed description of the LabView PID subroutine, see Reference 9.

The X PD Loop Structure takes the desired X position, specified by the user in the table coordinate system, and converts the position to the vehicle frame via a coordinate transformation subroutine called Convert to Vehicle Frame, Figure 64. The desired position, in the vehicle frame, is the set point input to the LabView PID subroutine. The process variable input, or instantaneous X position in the vehicle frame, is generated by the NPADS "star sensor" camera via a Vision subroutine called Vision Subsystem. In addition, the current position is routed through another coordinate transformation, Figure 65, for display in the table coordinate system on the User Control Panel.

The output from the LabView PID subroutine, or the controller action, is then routed to the Pulse Width Modulation (PWM) subroutine to control the individual thrusters. The direction of the controller action, or the sign of the PID subroutine output, is checked and routed to the appropriate PWM input line. Separate lines for positive and negative translation are required to ensure the appropriate thrusters are pulse width modulated. The Y PD Loop Structure is identical to the X PD Loop Structure. The Rotation PD Loop Structure differs in that the process variable input, or the current vehicle rotation angle, is fed back to the PID subroutine via the Rotation Angle Buffer vice the NPADS vision system.

The entire PD Control Structure segment is controlled through actuation of a push button switch, labeled PID control, on the User Control Panel. Following the successful completion of the Rate Sensor Bias calculation, the button is depressed and the vehicle is autonomously controlled.

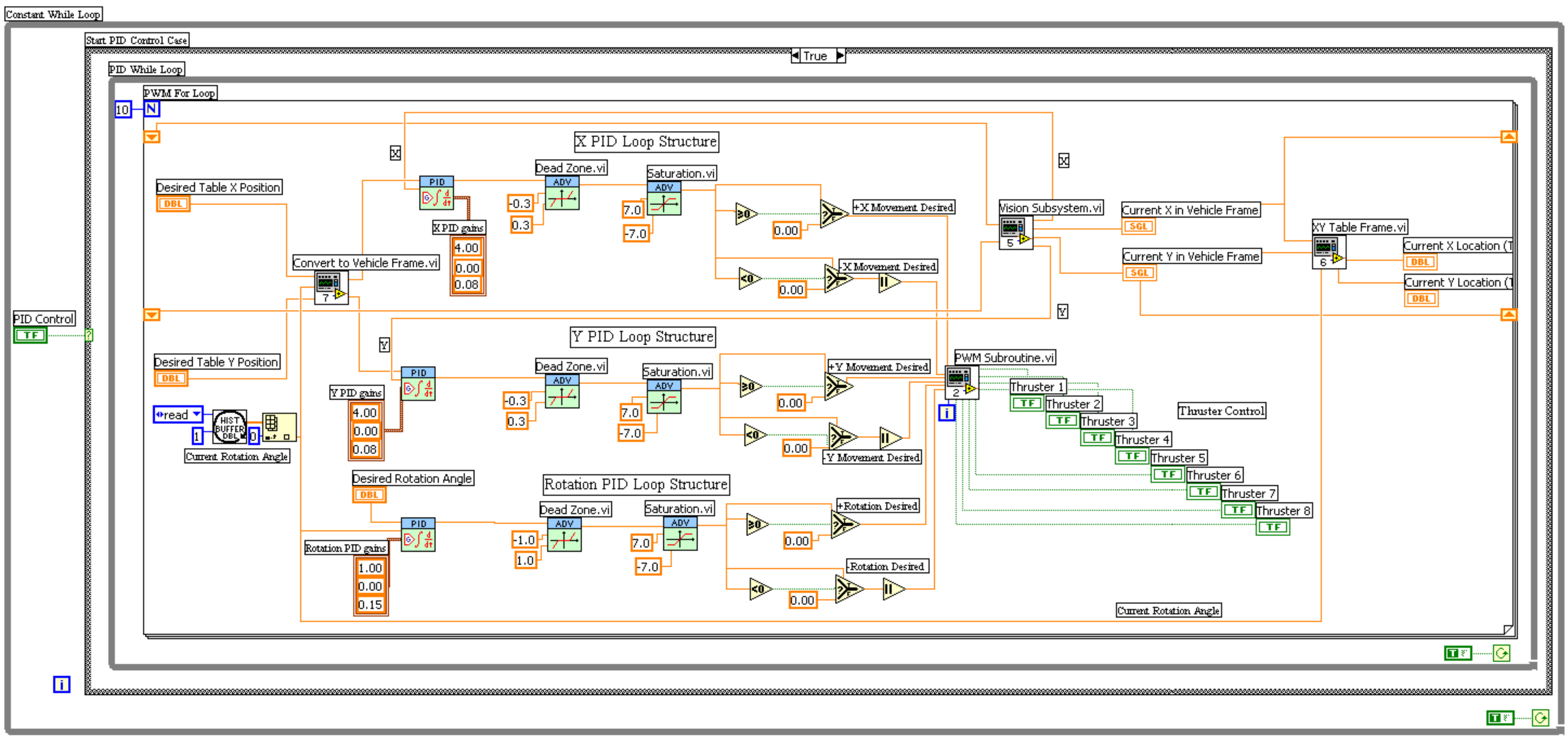

Figure 63 NPADS Autonomous Control PD Control Structure Segment

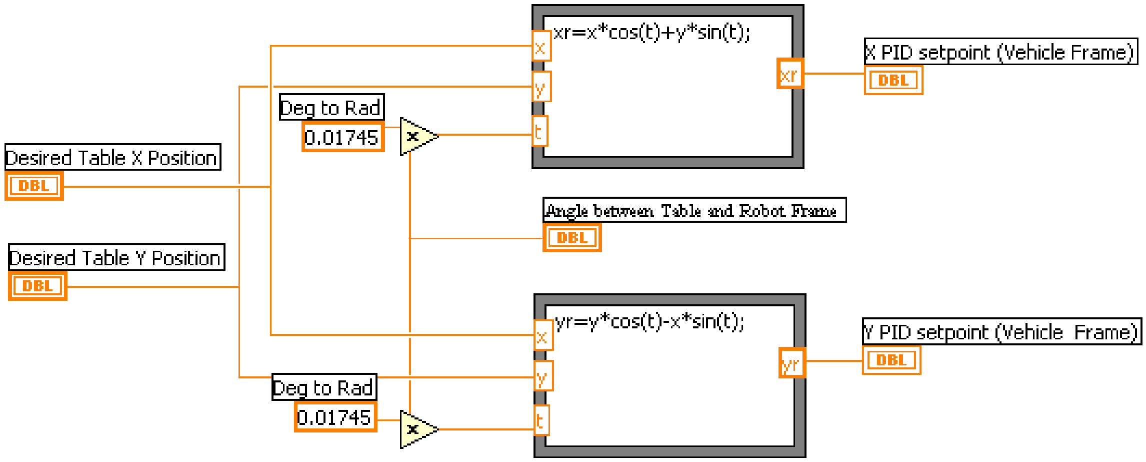

Figure 64 NPADS LabView Table-to-Vehicle Frame Conversion Subroutine

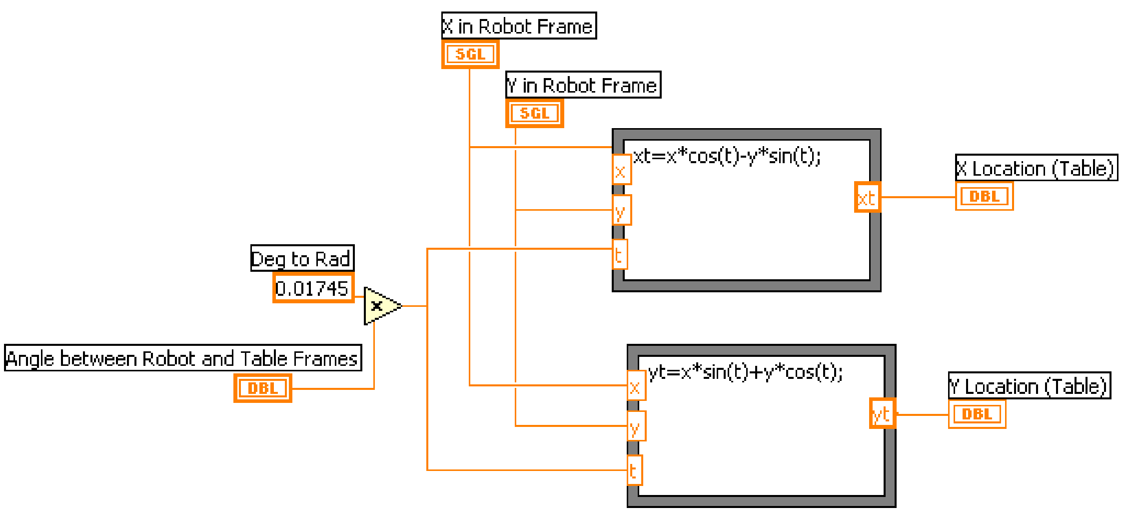

Figure 65 NPADS LabView Vehicle-to-Table Frame Conversion Subroutine

2. Pulse Width Modulation Subroutine

The Pulse Width Modulation subroutine, Figure 66, receives the controller action from the PID subroutines via six input lines, ±X, ±Y and ±Rotation. Each thruster on NPADS is used for a rotation and a translation in the positive or negative direction as described in Chapter IV. The input lines are routed to the appropriate thruster via a modulation block. Because two thrusters are used for translation and four thrusters for rotation, the modulation block uses the formula, $f = 0.5 \times (translationInput) + 0.25 \times (RotationInput)$, to determine the appropriate input modulation to the PWM comparator for each individual thruster. The comparator receives the input modulation and compares the value with the saw tooth carrier to produce the pulse width modulated thruster command.

The entire PD Control Structure segment is inside a PWM For loop. The saw tooth carrier waveform is created using the For loop counter which results in a waveform with an amplitude of 3 and frequency of 1.11 Hz. The carrier waveform is offset 0.1 to prevent excessive thruster chatter around zero. The pulse width modulated signal leaves the comparator in the form of a Boolean ON / OFF (True / False) command to the individual thruster. The thruster hardware is activated through a LabView Digital Write subroutine to the PXI 6713 card.

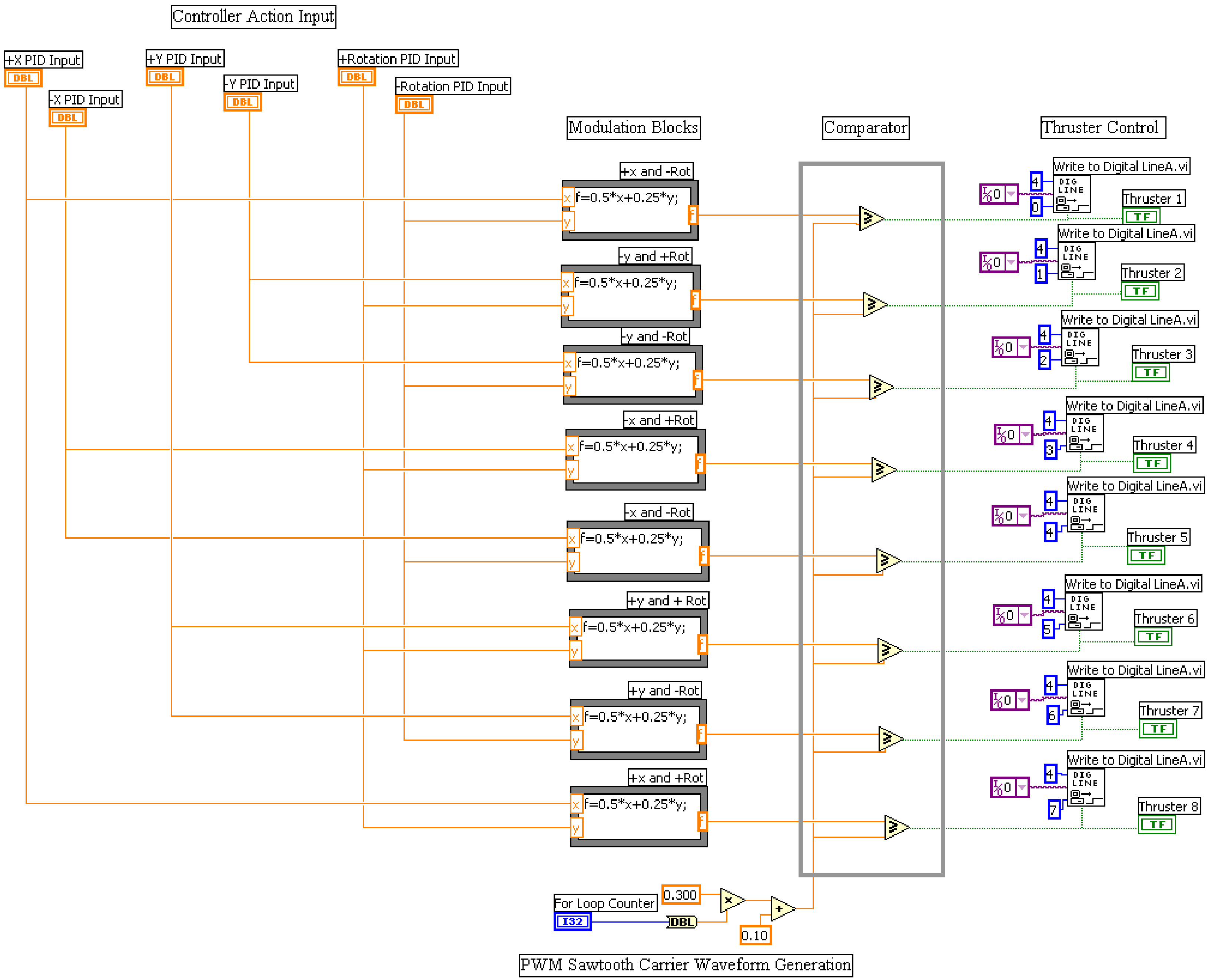

Figure 66 NPADS Pulse Width Modulation Subroutine

3. Vision Subroutine

The Vision Subroutine, Figure 67, uses the NPADS "star sensor" camera to locate a circular target on the ceiling above the NPADS operating table and fix the vehicle position in relation to the target. The subroutine uses built-in LabView IMAX vision subroutines to breakout the target from the background and provides a relative position in pixels. A summary of the IMAX vision subroutines used and the processing time is presented in Table 16. The relative position of the target in pixels is then converted to inches and passed to the X and Y PID subroutines of the PID Control segment.

Table 16 IMAX Vision Subroutines

Operation	Effect	Process Time (ms)
Threshold: Manual Threshold	All pixels outside the threshold value band 0 – 81 are set to zero, all others are set to 1.	2.0
Advanced Morphology: Remove Small Objects	Removes small, isolated noise using 1 iteration of a square, 8-connectivity filtering element	14.3
Advanced Morphology: Remove Borders	Removes objects touching the edge of the image	5.7
Particle Filter	Removes all objects with a Heywood Circularity Factor (the ratio of an object's perimeter to the perimeter of a circle of equal area) outside the range 0.8 to 1.2	40.3
Particle Analysis	Outputs the position of the center of the circle target, in pixels, from the upper left corner of the image. The LABVIEW VI built from this script translates the coordinates to provide (x,y) position, in pixels, from to the center of the image (camera boresight)	10.0

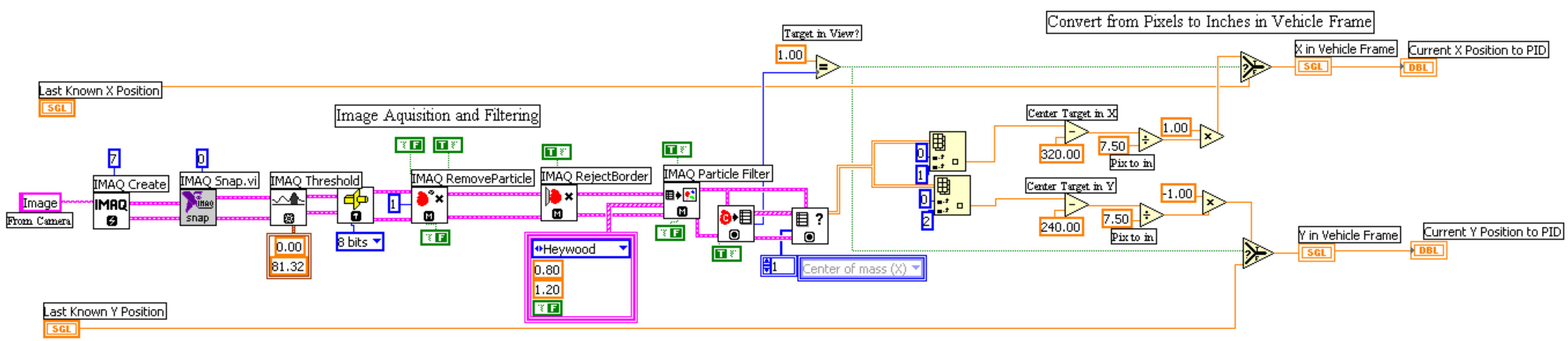

Figure 67 NPADS Vision Subroutine

THIS PAGE INTENTIONALLY LEFT BLANK

LIST OF REFERENCES

1. Jochim, David, "Mini AERCam: A Free-Flying Robot for Space Inspection," presentation to the Naval Postgraduate School, 22 February 2002.

2. AIAA 2002-4568, *Inertia Parameter Identification for a Free-Flying Space Robot,* by K. Yoshida and S. Abiko, p.1-6, 5 August 2002.

3. National Instruments, *NI 8171 Series User Manual,* August 2001.

4. National Instruments, *PXI E Series User Manual,* January 1999.

5. National Instruments, *6711/6713/6715 User Manual,* December 1999.

6. National Instruments, *IMAQ PCI/PXI-1408 User Manual,* June 1998.

7. Sidi, M. J., *Spacecraft Dynamics & Control: A Practical Engineering Approach,* pp. 260-289, Cambridge University Press, 1997.

8. Ullman, M. A., *Experiments in Autonomous Navigation and Control of Multi-Manipulator, Free-Flying Space Robots,* Ph.D. Dissertation, Stanford University, 1993.

9. National Instruments, *PID Control Toolset User Manual,* November 2001.

THIS PAGE INTENTIONALLY LEFT BLANK

INITIAL DISTRIBUTION LIST

1. Defense Technical Information Center
   Ft. Belvoir, Virginia

2. Dudley Knox Library
   Naval Postgraduate School
   Monterey, California

3. Department Chairman
   Department of Aeronautics and Astronautics
   Monterey, CA

4. Department of Aeronautics and Astronautics
   Professor Michael G. Spencer
   Naval Postgraduate School
   Monterey, CA

5. Department of Aeronautics and Astronautics
   Professor Brij N. Agrawal
   Naval Postgraduate School
   Monterey, CA

6. LCDR Robert D. Porter, USN
   Dallas, TX